

Review

A Review on Tailoring Stiffness in Compliant Systems, via Removing Material: Cellular Materials and Topology Optimization

Mauricio Arredondo-Soto ^{1,2,†} , Enrique Cuan-Urquizo ^{1,2,*,†}  and Alfonso Gómez-Espinosa ^{1,*} 

¹ Tecnológico de Monterrey, School of Engineering and Sciences, Querétaro 76130, Mexico; A00831724@itesm.mx

² Laboratorio Nacional de Manufactura Aditivay Digital (MADIT), Apodaca, Nuevo León 66629, Mexico

* Correspondence: ecuanurqui@tec.mx (E.C.-U.); agomez@tec.mx (A.G.-E.); Tel.: +52-442-238-3302 (A.G.-E.)

† These authors are part of the Metamaterials Lab Group at Tecnológico de Monterrey Campus Querétaro.

Abstract: Cellular Materials and Topology Optimization use a structured distribution of material to achieve specific mechanical properties. The controlled distribution of material often leads to several advantages including the customization of the resulting mechanical properties; this can be achieved following these two approaches. In this work, a review of these two as approaches used with compliance purposes applied at flexure level is presented. The related literature is assessed with the aim of clarifying how they can be used in tailoring stiffness of flexure elements. Basic concepts needed to understand the fundamental process of each approach are presented. Further, tailoring stiffness is described as an evolutionary process used in compliance applications. Additionally, works that used these approaches to tailor stiffness of flexure elements are described and categorized. Finally, concluding remarks and recommendations to further extend the study of these two approaches in tailoring the stiffness of flexure elements are discussed.

Keywords: cellular materials; topology optimization; flexure element; compliant system; tailoring stiffness



Citation: Arredondo-Soto, M.; Cuan-Urquizo, E.; Gómez-Espinosa, A. A Review on Tailoring Stiffness in Compliant Systems, via Removing Material: Cellular Materials and Topology Optimization. *Appl. Sci.* **2021**, *11*, 3538. <https://doi.org/10.3390/app11083538>

Academic Editor: Valentino Paolo Berardi

Received: 21 March 2021

Accepted: 9 April 2021

Published: 15 April 2021

Publisher's Note: MDPI stays neutral with regard to jurisdictional claims in published maps and institutional affiliations.



Copyright: © 2021 by the authors. Licensee MDPI, Basel, Switzerland. This article is an open access article distributed under the terms and conditions of the Creative Commons Attribution (CC BY) license (<https://creativecommons.org/licenses/by/4.0/>).

1. Introduction

Compliance is the term used when referring to low levels of stiffness, in other words, when flexibility is the characteristic feature. Compliant systems can be categorized in compliant mechanisms (Figure 1a), compliant joints (Figure 1b), and flexure elements (Figure 1c). Compliant mechanisms transmit motion, force, and energy through the elastic deformation of flexible members known as flexures. Compliant joints are the key-components in compliant mechanisms; they act analogously to the kinematic pairs in rigid-body mechanisms. The basic form of a compliant joint is a single flexure, which is usually formed by removing material from a bulk piece. A compliant joint can be composed of more than one flexure and could be considered as a compliant mechanism on its own. Flexures stretch, bend, or twist during deformation, which leads to the relative motion between parts in a compliant system.

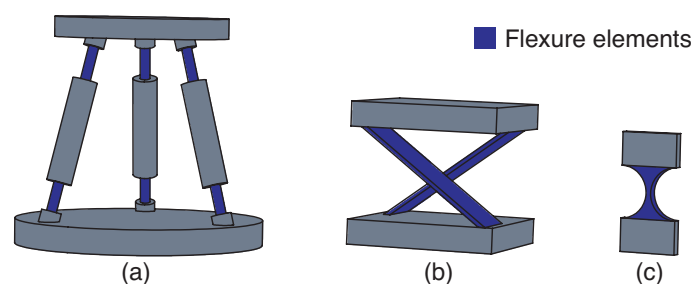


Figure 1. Compliant systems: (a) compliant mechanism, (b) compliant joint, and (c) flexure.

Compared with traditional rigid-body mechanisms, compliant mechanisms have many inherent advantages, including elimination of sliding contact between surfaces, monolithic manufacturing, higher precision, reduced friction, and reduced weight [1]. In contrast to their rigid-body counterparts, compliant mechanisms facilitate smooth, continuous motion, without backlash, and with high levels of repeatability and precision [2]. Therefore, compliant mechanisms find applications in fields requiring high precision motion, such as precision manufacturing [3], biological cell handling [4], micro/nano-manipulation [5], positioning stages [6], microelectromechanical systems (MEMS) [7], micro-vibration suppression [8], optical guides [9], and so forth.

Apart from the advantages, compliant systems have some drawbacks owing to their intrinsic coupling of kinematics and elastomechanical behaviors. Consequently, design and analysis cannot be done by separating kinematics and dynamics. The design process is even more complicated if the compliant elements undergo large deflections, due to the resulting nonlinear relationship between stress and strain. The challenging process for designing and analyzing compliant systems limits the wide use of three-dimensional (3D) architectures with multi Degrees of Freedom (DoFs), restricts the design to small deflections, and may lead to inaccuracies such as cross-coupling errors and erroneous undesired displacements termed as parasitic motions [10–13].

Applications increasingly demand compliant systems with large workspaces, multiple-DoFs, low cross-coupling errors, and reduced parasitic motions. Attempts to reduce inaccuracies and limitations have been proposed, some examples are the use of redundant constraints [14,15], compound joints [16,17], addition of subsystems [18,19], implementation of tracking control systems [20], and design of spatial complex architectures to perform basic planar motions [21]. However, all of these techniques are based on the incorporation of elements or sub-systems to the compliant system, thus increasing complexity, size, and weight.

The performance of a flexure element, i.e., its range of motion, accuracy, kinematics, and dynamics, is determined by the proper characterization of its force-deformation relation, i.e., the stiffness (or compliance) of the element. Having control over the stiffness of the flexure elements appears as an ideal way to deal with inaccuracies and limitations of compliant systems. As the stiffness of a flexure element is governed by the material that composes it, boundary conditions and external geometry, changing its dimensions will result in a modification to its stiffness. However, the geometry is generally dependent on the available material stock, manufacturing process, or other design constraints [22]. Moreover, a change in the overall dimensions of a flexure element may lead to a loss in the off-axis stiffness leading to instability, thus resulting in inaccuracies.

In this regard, methods to control the stiffness of flexure elements that do not imply a radical change in their overall dimensions can be found in the literature [23,24]. Some methods, such as static balancing [25–30], antagonism principle [31,32], and lever mechanism [33–35], consist of pre-deforming the flexure elements of compliant systems, reducing actuation effort, thus increasing range of motion. Flexure elements used in these methods are commonly coil springs. Others techniques are based on changing the effective length of elastic components in a compliant system to achieve variable stiffness [36–40]. Despite the success in modifying the stiffness via pre-deformation or change in effective length of flexures, the use of external systems or actuators is demanded, thus increasing complexity, size, and cost.

Intentional contact between elements in compliant systems is another approach to modify their stiffness known as contact-aided. Besides, as contact surfaces are common parts of the compliant systems, this method avoids the use of external elements and actuators. Examples of contact-aided compliant systems can be found in the literature, addressing topics such as morphing [41–43], stress relief [44–46], improve load-bearing capacity [47], and energy absorption [48,49]. In all cases, global strain capability of contact-aided compliant systems is increased. Furthermore, in [50,51] variable stiffness compliant joints are achieved through changing the effective length during deformation by self-contact between the flexible parts and support points manufactured as part of the same system.

Contact-aided compliant systems act as stiffness switches during deformation and are suitable only in applications where abrupt changes of stiffness are needed.

Approaches to tailor the stiffness of compliant systems based on selectively removing material from flexure elements maintaining their overall dimensions appear as the possible solution to deal with inaccuracies and limitations of compliant systems. These approaches termed as Cellular Materials and Topology Optimization allow an accurate modification of the stiffness of flexure elements avoiding the use of external elements and actuators. Tailoring stiffness via Cellular Materials is based on using predefined periodic arrays combining material and void spaces to substitute the flexure elements of compliant systems [22]. The process to tailor the stiffness of a flexure element via Cellular Materials is graphically explained in Figure 2a.

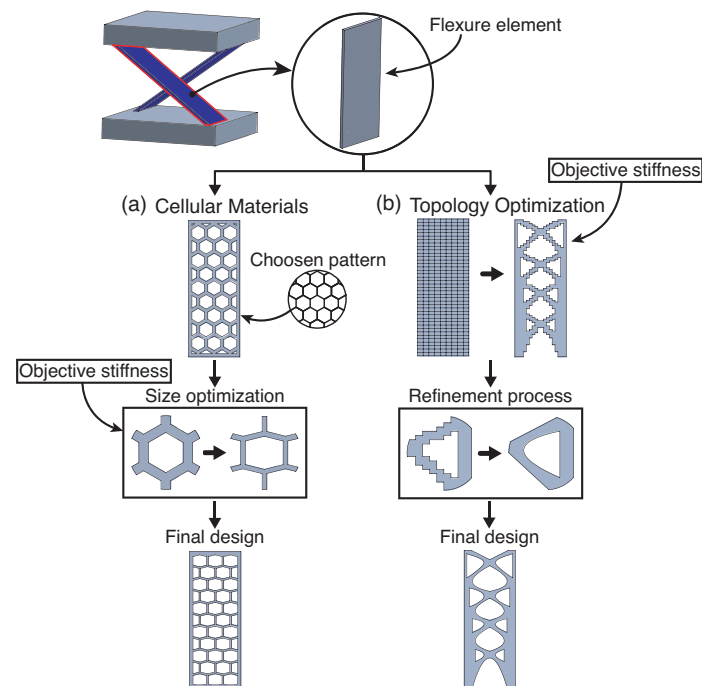


Figure 2. Process to tailor stiffness of flexure elements via (a) Cellular Materials and (b) Topology Optimization (Figure based on that in [52]).

Topology Optimization has been widely used in the design and synthesis of compliant systems [53,54], and even to obtain specific stiffness values [55]. However, the resulting compliant systems often have complex architectures and distributed compliance, thus leading to complicated analysis, manufacture, and further implementation. Therefore, recent efforts have been focused on applying Topology Optimization processes only in the flexible parts (flexures) of compliant systems allowing an acceptable characterization of the stiffness while maintaining original system macro-shape and thus manufacturability. Then, tailoring stiffness via Topology Optimization consists of removing material from flexure elements based on a goal function [56]. The process to tailor the stiffness of a flexure element via Topology Optimization is graphically explained in Figure 2b. Both techniques are intimately related, as shown in Figure 2, as to achieve the optimal configuration of the cellular structure, it is necessary to perform an optimization process commonly called size or shape optimization, and the result of a Topology Optimization process after a post-processing refinement is often a cellular structure. Optimization via cellular materials is often done intuitively and manually, while Topology optimization is automated via computational algorithms.

While both Cellular Materials and Topology Optimization can be reviewed independently for other applications, here we focused on tailoring stiffness via these two approaches acting at flexure level that has applications in compliant systems. The con-

trolled distribution of material within a certain structure often leads to several advantages; one of them is the customization of the resulting mechanical properties of it. Following these two approaches, this can be achieved; therefore, reviewing the related literature to aid the understating and implementation of the approaches gains relevance. The main effort of this work is in clarifying how the stiffness can be tailored through these approaches and reviewing the works found in the literature that used them on flexure elements. Comments on the mechanical characteristics that the compliant systems gained with these methods, such as weight reduction, stiffness ratios, stress relief and motion range, are also addressed. As this work focuses on tailoring stiffness, applications of these methods in the customization of properties, such as thermal [57], electrical [58], and acoustic [59], are beyond of the scope of this review. This review is structured as follows. Tailoring stiffness via Cellular Materials is presented in Section 2. Tailoring stiffness via Topology Optimization is detailed in Section 3. Concluding remarks and discussion on research trends of these two are given in Section 4.

2. Tailoring Stiffness via Cellular Materials

Cellular Materials are essentially patterns that, in contrast to their homogeneous counterparts, are heterogeneous materials that have a unit-cell and repetition which leads to a structured distribution of material and voids [60]. Cellular Materials can be random or periodic, the latter are defined by a unit-cell that is repeated (combining material and voids). Therefore, a cellular solid is one made up of an interconnected network of solid struts or plates which form the edges and faces of cells. Typical cellular structures are shown in Figure 3. Two-dimensional (2D) patterns are called honeycombs (Figure 3a). 3D Cellular Materials are called foams and can be open- and closed-cell (Figure 3b,c).

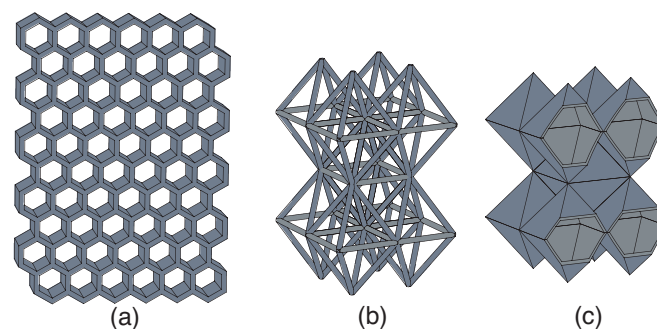


Figure 3. Typical cellular structures: (a) 2D cellular structure known as “Honeycomb”, (b) 3D open-cell structure (lattice structure), and (c) 3D closed-cell structure. The structures in subfigures (b,c) are 3D structures termed as “Foams”.

Commonly, open-cell structures are those where the void space is interconnected with a network of slender struts (open-cell structures can also be composed of surface shells, such as gyroids [61,62]); these types of Cellular Materials are among the most popular choices in design and are commonly called lattice structures, or simply lattices [63], an example of a 3D lattice is shown in Figure 3b. On the other hand, closed-cell structures are those where the network consists of interconnected surfaces that separate voids by cell walls or membranes, an example of a 3D closed-cell Cellular Material is shown in Figure 3c.

Cellular Materials are designed to offer advantages that cannot be afforded by homogeneous structures, such as the ability to locally tune properties, add multi-functionality, and improve performance while maintaining structural integrity and decreasing weight [64]. Due to their great stiffness-weight ratio, lattice structures have been used extensively in lightweight applications to reduce mass while maintaining or even increasing stiffness levels [65–68]. Most of these works used an optimization process (often called size and shape optimization) to select the most efficient configuration of unit-cell, dimensions of struts elements of the lattice, and the best way to infill bodies with this lattice. All of these processes have the aim of achieving substantial mass reduction and high structural stability while ensuring manufacturability.

When the characteristic lattice dimensions are significantly smaller than the overall dimensions of a piece of solid, one can represent the properties of such structural solids by means of apparent properties considering them as homogeneous having equivalent continuum properties [69]. In general, an apparent property, $\langle P \rangle$, of a Cellular Material is often expressed as $\langle P \rangle = CP\bar{\rho}^n$, where P is the property of the parent material (e.g., Young's modulus), and n and C are constants related to the *deformation mechanism* of the lattice elements and topology. The exponent n , which depends on the micro-architecture response, defines the scaling relation of the apparent property with the relative density [70]. The relative density is equal to the volume fraction, $\bar{\rho} = V_s/V_c$, where V_s is the volume of the solid material and V_c is the volume of the lattice material considering the external dimensions.

According to their deformation mechanism, cellular Materials are classified into two main groups: bending-dominated and stretch-dominated structures [71]. When loaded, the cellular elements of the structured material can respond by bending or stretching-shortening; thus, they are said to be bending- or stretch-dominated (Figure 4a,b), respectively. Therefore, customization of the stiffness via Cellular Materials is possible as their apparent mechanical properties show dependence on the following: (i) the mechanical properties of the parent material, (ii) the topology and cell geometry, and (iii) the relative density. Properly planned selection or modification on any of these three can lead to a meta-material with tailored properties. In this regard, the stiffness of a compliant system can be modified through the implementation of specific cellular arrays in the flexible parts of the system.

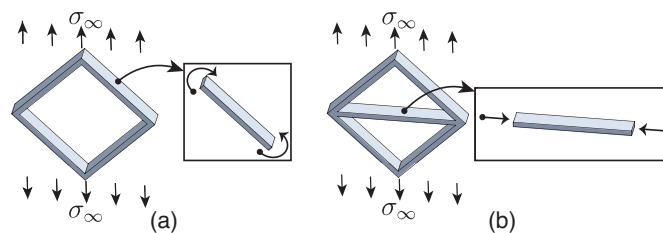


Figure 4. Schematic of (a) bending-dominated and (b) stretch-dominated structures.

Tailoring stiffness has become more relevant with the emergence of modern manufacturing processes such as additive manufacturing techniques, capable of fabricating complex topologies and shapes [72–75]. Some studies [76–78] showed how the stiffness in beams can be customized by using different types of cellular structures while obtaining minimum weight designs. Other works [79–81] focused on obtaining optimal designs of lattice structures to achieve the desired stiffness along with exceptional load-bearing efficiency and minimum weight. Later, Maskery et al. [82] investigated the effect of cell topology, orientation, and volume fraction to provide a specified stiffness in the lattice structures. Further, Weisgraber et al. [83] conducted research works where they proved that by modifying cell parameters, it is possible to control the stress-strain curve of a Cellular Material to assess specific load requirements and performance. A similar study was developed by Wang et al. [84], where the authors optimized lattice structures to provide specific stiffness for given multi-loading scenarios in the low volume fraction limit. Most recently, Alvarez-Trejo et al. [85] synthesized a new type of Bézier-based metamaterial, characteristics of which enable the generation of structures with customized mechanical properties by adjusting the geometry of the unit cells.

Some studies [86–90] demonstrated the possibility to tailor specific stiffness depending on the loading direction, allowing the design of customized anisotropic Cellular Materials. Niknam et al. [87] introduced the concept of multi-directional functionally graded Cellular Materials made by assembling porous unit cells of dissimilar densities and cell topologies to improve the performance of lightweight structural elements. In [88], the authors evidenced that tailoring the apparent anisotropy in Cellular Materials at the macroscopic level is possible by changing the ratio of bending-to-axial stiffness of the constituent beams, as, depending on the direction of loading, the nature of the mechanical response of cubic elementary trusses changes smoothly from bending-dominated to stretching-dominated.

This concept was also studied in [86], where the authors performed customization of effective anisotropic material properties in micro-lattice structures by controlling the unit-cell topology. Recently, Chen et al. [90] designed isotropic Cellular Materials created by superimposing complementary anisotropic lattices, enhancing the potential of high-stiff isotropic Cellular Materials. Variable stiffness is also achieved by including contacts during deformation of Cellular Materials. An example is found in Tanaka et al. [91], where the authors synthesized a square-cell Cellular Material with the bi-stiffness property in response to compressive loading. The specific case of stiffness depends on the orientation of the unit cells leading to a specific deformation of cells and further overlapping of cell walls. Kim et al. [89] synthesized a 3D variable stiffness and dual Poisson's ratio Cellular Material by including internal contacts between slit surfaces during both tensile and compressive loading achieving engineered stiffness.

Applications of tailored Cellular Materials have been focused mainly on stiffness maximization. Examples of Cellular Materials customized to offer maximum possible stiffness using different cellular structures such as 2D honeycombs [92,93], 3D lattices [94,95], and 3D closed-cell foams [96] are found in the literature. Tailored Cellular Materials have been also used to maximize transverse shear stiffness in honeycomb cores [97,98]. Studies of applications including the use of Cellular Materials to enhance buckling behavior [99], tune stress localization, minimize stress levels [100], and engineer failure location for specific load conditions [101] are limited.

Optimization via Cellular Materials can also be used for match specific stiffness. This aspect is particularly attractive for the manufacturing of bone implants, where the elastic modulus of the implant should match that of the bone in order to avoid stress shielding effects, bone atrophy, and implant loosening. Additionally, offering advantages such as improving stability by promoting tissue ingrowth and high energy absorption to withstand impacts. Three-dimensional topologies are the most frequently encountered in this application. A variety of works for this application can be found in the literature. Parthasarathy et al. [102] presented a thorough review where they expose the capacity of additive manufacturing techniques to fabricate biomedical devices with mechanical properties of surrounding bone tissue with replacements parts.

Most recently, tailoring stiffness through Cellular Materials to enhance flexibility or compliance behavior has been studied. Some of the first examples can be found in the works of Kim et al. [103,104], where the authors proposed Cellular Materials with customized anisotropic stiffness. The proposed materials consisted of flexible mesostructures designed from the deformation of re-entrant auxetic (negative Poisson's ratio) honeycomb and compliant amplifiers mechanisms. They could tailor in-plane properties of the said mesostructures, obtaining low stiffness and high strain in one direction and high stiffness and low strain in the other direction. A complete review of auxetic cellular materials is found in [105]. After, Duoss et al. [106] demonstrated the possibility to independently tailor compression and shear response in 3D printed Cellular Materials offering the extremal property of negative shear stiffness in designed structures. Then, Neff et al. [107] used modified diamond lattice structures to create Cellular Materials with reduced stiffness, advantageous for energy absorption, vibration isolation, and reduction of stress. Later, Runkel et al. [108] modified the topology of hexagonal chiral lattices and demonstrated that purposely choosing the parameters permits to tailor the behavior of the chiral lattice, enabling extreme variations in stiffness, including the possibility to attain negative and zero-stiffness regimes over large compressive strains which exemplifies the potential to tune deformation of compliant systems. Additionally, Ion et al. [109] introduced the meta-material mechanisms concept, which considers cellular materials as machines instead of materials and allows the creation of macroscopic movement through the well-defined interaction of cells in a single block of cellular material. Similarly, Ou et al. [110] presented a group of auxetic-inspired material structures that can transform into various shapes upon compressive loading. Most recently, in [111] a 2D kagome honeycomb was optimized for delivering high amplitude actuation. In the same year, Dunn et al. [112] demonstrate that

changing the cell size in lattice materials might involve maximizing stiffness in one mode while minimizing it in another.

Regarding this, some applications have taken advantage of the compliance behavior offered by Cellular Materials. One of the most extensively studied applications is in shape morphing as the material used should not only be in-plane flexible enough to morph with actuation, but stiff enough not to deform excessively under out-of-plane loads. To this end, 2D cellular structures have been suggested for general morphing skin applications [113–115]. In [113], the authors presented a novel zero-Poisson's ratio honeycomb structure that can achieve deformations along two orthogonal directions and avoid the increase of effective stiffness in the morphing direction by restraining the Poisson's effect in the non-morphing direction. The same concept was explored by Liu et al. [114,115] in the development of zero-Poisson's ratio cellular structures with lightweight, low in-plane moduli and high strain capability. Results demonstrated the potential of the proposed structures for in-plane morphing. Moreover, the main application is in aircraft morphing, where efforts have been mainly focused in airfoil-core morphing [116–119] and airfoil-skin morphing [120–126]. Bornengo et al. [116] proposed the use of an auxetic hexagonal structure as the airfoil-core of wings as an attempt to take advantage of the high deformability of the structure thus providing the flexibility required for morphing, while preserving the structural integrity due to its high in-plane shear resistance. Dong et al. [117] designed airfoil-cores with a re-entrant cellular structure due to their ability to undergo large in-plane displacements with limited deformation in span-wise direction. Zhang et al. [118] investigated the use of a cross-shaped honeycomb structure in airfoil-core morphing, resulting in great in-plane deformation capacity and adequate out-of-plane support. Heo et al. [119] investigated the airfoil-core morphing capacity of three types of Cellular Materials through the in-plane flexible properties. Hexagonal chiral, regular honeycomb, and re-entrant honeycomb were chosen for this analysis. All structures showed high levels of in-plane flexibility. The re-entrant honeycomb showed the highest flexibility and causes a lower stress in cell walls than the other cellular cores, thus suggesting potential to be used in real morphing applications. On the other hand, Olympio et al. [120] studied the use of hexagonal honeycomb cellular structures in airfoil-skin morphing. Results showed that Cellular Materials could easily undergo global strains several times greater than the parent material while maintaining good out-of-plane stiffness; however, when honeycomb Cellular Materials are stretched along the principal axis they geometrically stiffen, thereby reducing the maximum global strain achievable. Olympio et al. [121] proposed two types of zero-Poisson's ratio cellular structures (hybrid and accordion) to be used in one-dimensional airfoil-skin morphing applications. Results showed that the axial stiffness in the motion direction of the zero-Poisson's ratio cellular structures remains low when the skins are restrained in the non-morphing direction, making these cellular structures ideal for use in airfoil-skin morphing. Other works [122–124] have studied similar zero-Poisson's ratio cellular structures to be used in airfoil-skin morphing, obtaining high levels of flexibility in the actuation direction while maintaining the desired shape and strength in the others. Most recently, in [125,126] a new Cellular Material with zero-Poisson's ratio called Fish cell (Figure 5b) was introduced for applications in airfoil-skin morphing. The proposed cellular structures were parametrized to obtain desired stiffness values under specific conditions.

Finally, 3D arrays have been reserved for complete wing morphing [127,128]. 2D cellular structures used in airfoil-core and airfoil-skin morphing can be subdivided in three main categories according to the value of their Poisson's modulus (ν): positive-Poisson ($\nu > 0$), zero-Poisson ($\nu \approx 0$), and auxetic ($\nu < 0$). A complete overview of airfoil morphing by 2D cellular structures is depicted in Figure 5a, graphically showing the main categories of 2D patterns: positive-Poisson, zero-Poisson, and auxetic. In general, 2D cellular structures used in airfoil morphing applications showed lower levels of in-plane stiffness than their parent material, and higher levels of out-of-plane stiffness than fully dense elements of comparable mass, as well as mass reduction percentages above 90% and higher strain capabilities [120]. In airfoil cores, auxetic cellular structures are preferred due to their higher in-plane flexibility which causes lower stress in cell walls than other types of

cellular cores [119]. On the other hand, airfoil-skin morphing commonly uses sandwiched skins with cellular structure cores and thin, high-strain-capable face sheets that provide a smooth aerodynamic surfaces. However, this sandwich configurations also involve dealing with the boundary effects and Poisson’s contractions or expansions. Therefore, zero-Poisson cellular structures are preferred to deal with this restriction in unidirectional morphing applications such as airfoil-skin morphing.

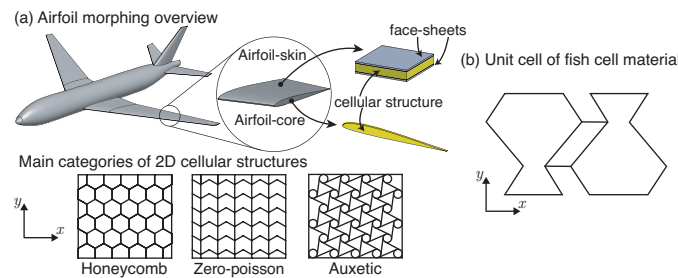


Figure 5. (a) Complete schematic overview of airfoil morphing and main categories of 2D cellular structures, and (b) unit-cell of the zero-Poisson’s ratio cellular material termed as “Fish cell” (figure adapted from in [125]).

Tables 1 and 2 present the principal works of airfoil-core and airfoil-skin morphing applications using 2D Cellular Materials. Works in these tables are categorized by author and cellular structure used. Stiffness reductions are presented by in-plane Young’s modulus ratios, E_{cx}/E and E_{cy}/E , for airfoil-core morphing (see Table 1), and by main-direction Young’s modulus ratio, E_c/E , and shear-stiffness ratio, G_c/E , for airfoil-skin morphing (see Table 2), where E_c and G_c are the Young and shear moduli of the Cellular Material, while E is the Young’s modulus of the parent material. Additionally, the percentage of weight reduction is reported in Table 1. Tables 1 and 2 are presented to show the potential to perform high reductions of the stiffness levels in flexure elements through the substitution of fully dense solids with cellular patterns.

Table 1. Stiffness reduction via Cellular Materials: Airfoil-core morphing. Principal works found in literature by author and cellular structure used (P: positive Poisson, Z: zero-Poisson, A: auxetic). Young’s modulus ratios E_c/E between the obtained by the application of Cellular Material, E_c , and that of the parent material E for in-plane E_{cx}/E and E_{cy}/E stiffness, and percentage of weight reduction. “–” indicates that there is no sufficient information reported to obtain that parameter. The percentage of weight reduction was obtained based on the reported relative density $\bar{\rho}$ of the cellular structure.

Author	Cellular Structure	Young’s Modulus Ratios		Weight Reduction (%)
		$(E_{cx}/E) \times 10^5$	$(E_{cy}/E) \times 10^5$	
Bornengo et al. [116]	A—Hex. Chiral	1.18–0.60	1.18–0.60	90–95
Dong et al. [117]	A—Re-entrant	2.51	1.35	–
Zhang et al. [118]	P—Cross-shaped	0.25	0.13	–
Heo et al. [119]	A—Hex. Chiral	11.58	11.58	90
	P—Hexagonal	69.32	69.32	94
	A—Re-entrant	427.19	427.19	81

Table 2. Stiffness reduction via Cellular Materials: Airfoil-skin morphing. Principal works found in literature by author and cellular structure used (P: positive Poisson, Z: zero-Poisson, A: auxetic). Main direction Young’s modulus ratio E_{cx}/E , and shear stiffness ratio G_c/E . “–” indicates that there is no sufficient information reported to obtain that parameter.

Author	Cellular	Young’s Modulus Ratios	
	Structure	E_{cx}/E	G_c/E
Olympio et al. [121]	Z—hybrid	0.096–0.0047	–
	Z—Accordion	0.0047–0.10	–
Olympio et al. [120]	P—Hexagonal	$0.39\text{--}2.88 \times 10^{-5}$	$0.022\text{--}1.07 \times 10^{-5}$
Chen et al. [122]	Z—Chevron	$0.033\text{--}2.92 \times 10^{-5}$	$5.2 \times 10^{-5}\text{--}6.74 \times 10^{-4}$
Vigliotti et al. [123]	Z—Chevron	3.29×10^{-6}	2.05×10^{-2}
Chang et al. [124]	P—Hexagonal	0.015	0.0025
	Z—Accordion	0.023	0.0026
Zadeh et al. [125,126]	Z—Fish cell	$1.84 \times 10^{-6}\text{--}5.75 \times 10^{-7}$	1.30×10^{-7}

Other important application of the compliance behavior of Cellular Materials is in energy absorption. Cellular Materials are suitable for energy absorption applications as their particular structures permit high levels of elastic deflections without permanent deformations or high values of stress, allowing the material to spring back to its original configuration after the load is released. There are many works in the literature that prove the tailorability of Cellular Materials by manipulating their structural topology to enhance energy absorption capacity e.g., general energy absorption [129,130] or impact absorption [131–134]. Some studies generate negative stiffness materials [135,136], increasing the amount of energy absorbed, and others include contacts during the deformation of Cellular Materials to ensure restorability [137,138]. Many authors extensively studied the use of Cellular Materials in energy absorption applications, and a review of this application is out of the scope of this work. Therefore, interested readers are referred to specialized reviews in [139–142].

In the process of tailoring stiffness via cellular materials approach, certain topologies are preferred depending on the stiffness objective (increase stiffness or reduce stiffness). When stiffness maximization is the objective, a stretch-dominated lattice and closed cell structures are preferred. On the other hand, if flexibility is the goal, a bending-dominated auxetic and zero-Poisson’s ratio honeycombs are the most commonly used. The unit-cells of some of the most commonly used cellular structures for tailoring stiffness are shown in Figure 6. Increasing stiffness via cellular materials has been widely studied; therefore, unit cells for this objective, shown in Figure 6, are categorized in 2D-lattice structures, 3D-lattice structures, and Closed-cell structures. On the other hand, reducing stiffness via cellular materials has been limited to explore 2D-lattice structures; thus, unit cells for reduce stiffness, shown in Figure 6, are only in the category of 2D-lattice structures, nevertheless, they are separated according to their Poisson’s ratio behavior in positive Poisson’s ratio, auxetic, and zero-Poisson’s ration.

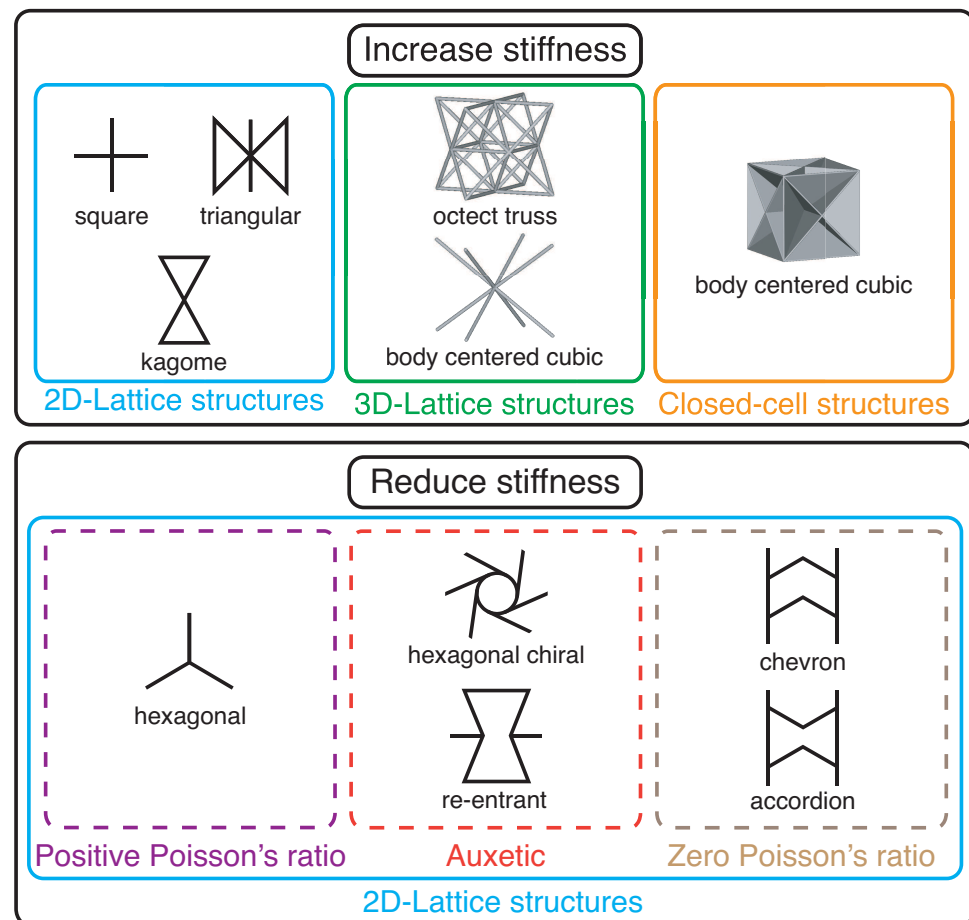


Figure 6. Unit cells of some of the most commonly used cellular structures for tailoring stiffness. Unit cells for increase stiffness are categorized in: 2D lattice structures (square [92], triangular [93], and kagome [100]), 3D-lattice structures (octet truss [94], and body centered cubic [81]), and closed-cell structures (body centered cubic [96]). Unit cells for reduce stiffness are only in the category of 2D lattice structures, and they are separated according to their Poisson's ratio behavior in: positive Poisson's ratio (hexagonal [119]), auxetic (hexagonal chiral [116], and re-entrant [117]), and zero Poisson's ratio (chevron [122], and accordion [121]). Some of the unit cells were generated using nTopology[®].

Additionally, to address properly the problem of tailoring stiffness via cellular materials, it is convenient to follow the next guideline. First, define the stiffness objective (increase or reduce stiffness). Then, identify the appropriate cellular material, for which it is necessary to identify the desired deformation mechanism (bending-dominated or stretch-dominated) and select an adequate topology (honeycomb, closed-cell structure, or open-cell structure). After, adjust the unit-cell parameters (geometry and relative density) to modify the stiffness of the cellular material. Afterward, compare the obtainable stiffness with the stiffness objective and evaluate if the cellular material is adequate. Next, if the objective stiffness is achieved, then the final step is the implementation. On the other hand, if the objective stiffness is not be achieved with the selected cellular material, then return to the topology identification step and repeat the process. The above-mentioned guideline is summarized in the diagram shown in Figure 7.

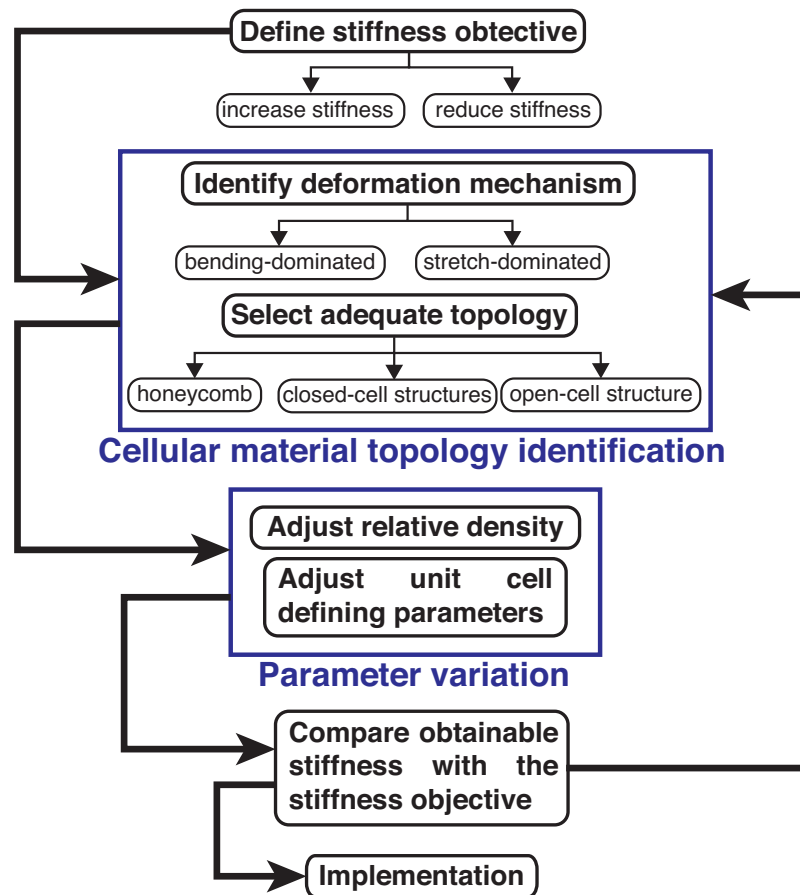


Figure 7. Guideline diagram to select an appropriate cellular material for tailoring stiffness.

Cellular Materials in Compliant Systems as Flexure Elements

There is a great amount of evidence for the capability of Cellular Materials to achieve desired levels of compliance in certain directions while maintaining high levels of stiffness in others. However, only Merriam and Howell [22] have applied a cellular lattice structure directly in the flexures elements of compliant joints, as shown in Figure 8. In [22], Merriam and Howell introduced the concept of *lattice flexure*, which was not common before additive manufacturing techniques were widely available. They demonstrated that these types of flexures have a reduced bending stiffness when compared to traditional rectangular-section blade flexures of similar dimensions while maintaining comparable stiffness in off-axis directions. Making use of additive-manufactured flexures, they found that both type of lattice flexures—X-type and V-type—shown in Figure 8 have the potential to reduce the bending stiffness by 60–80% compared to a traditional blade flexure of similar size, and at the same time to exhibit a torsional/bending stiffness ratio as much as 1.7 times higher than an equal aspect-ratio blade flexure, and a transverse bending/motion-direction bending stiffness ratio up to 6.5 times higher than an equal aspect-ratio blade flexure.

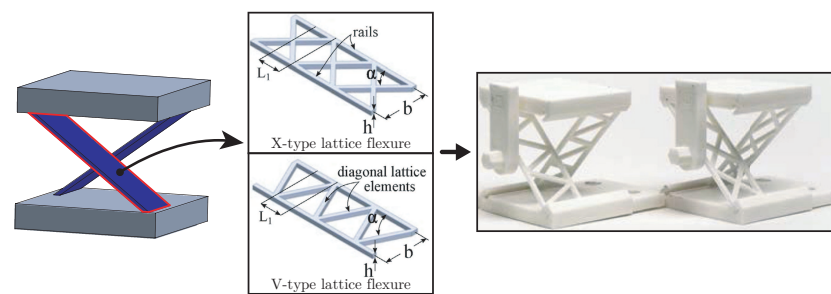


Figure 8. Lattice flexures proposed by Merriam and Howell [22] to be used in cross-axis flexural joints. (Adapted with permission from ref. [22]. 2021, Elsevier.)

Aiming to modify or allow compliance, it is possible to tailor the stiffness of flexure elements via Cellular Materials, while obtaining other advantageous mechanical conditions such as mass reduction, stress relief, and increments in stiffness ratios. However, when specific stiffness values are desired, tailorability is possible by using optimization processes that modified the final configuration of predefined cellular structures (see Figure 2). Then, one may express the effective stiffness as a function of cell parameters (strut or wall thickness, length, width, angle, etc.). Although this approach to design is powerful, its disadvantage is that the true optimization of the resulting materials architecture is ultimately limited by the designers initial choice of cellular structure. Therefore, other types of optimization processes that overcome this limitation are reviewed in the following section. This approach, termed as Topology Optimization, results in the optimal topology by removing or adding material to a design domain.

3. Tailoring Stiffness via Topology Optimization

Topology Optimization is a computational design method, which varies the material distribution within a structure or part, considering a predefined performance objective. In contrast to size and shape optimization in the use of Cellular Materials, topology optimization does not require a predefined initial design, and it can generate optimal geometries when intuitive design approaches fail [143]. The general Topology Optimization problem can be described as follows: To find the material distribution that minimizes an objective function F , subjected to a volume constraint $g_0 \leq V_0$ and possibly n other constraints $g_i \leq 0, i = 1, \dots, n$. The material distribution is described by the density variable $\bar{\rho}(x)$ that can take any value among 0 (void) and 1 (solid material) at any point in the discretized design domain Ω . This optimization problem can be written in a mathematical form as

$$\begin{aligned}
 \min_{\bar{\rho}} : & F(\bar{\rho}) \\
 \text{s.t.} : & g_0 \leq V_0 \\
 & : g_i(\bar{\rho}) \leq 0, \quad i = 1, \dots, n \\
 & : \bar{\rho}(x) = \text{value among 0 and 1} \quad \forall x \in \Omega.
 \end{aligned} \tag{1}$$

Considering the density approach, this Topology Optimization problem is typically solved by discretizing the domain Ω into m finite elements and density can take either the value 0 or 1. In this case, the last line of Equation (1) must be rearranged as $\bar{\rho}_j = 0$ or 1 for $j = 1, \dots, m$. On the other hand, the continuous Topology Optimization problem allows the finite elements to take values between 0 (void) and 1 (solid material). In this case, the last line of Equation (1) is reformulated as $0 \leq \bar{\rho}_j \leq 1 \quad j = 1, \dots, m$.

In general, Topology Optimization approaches are density-based and level set-based. In density-based methods [144], which include the popular Solid Isotropic Material with Penalization (SIMP) method [145], the geometry composed of finite elements is described via a material distribution of two or more phases, of which usually one represents “no material” (i.e., the void phase) leading to jagged boundary geometries. On the other hand, level set-based methods [143] define the interfaces between material phases implicitly by iso-contours

of a level set function allowing a crisp description of the boundaries and the accurate enforcement of boundary conditions. For further details on Topology Optimization methods, solution strategies, algorithms, regularization methods, etc. refer to the works in [146–149].

Thus, by selecting a specific objective function F in Equation (1), it is possible to create structures with customized properties, e.g., stiffness. When the design domain has a simple geometry and is free of specific boundary conditions, the topology-optimized result is often a cellular pattern [56] (Figure 2b). In addition, structures resulting from Topology Optimization processes need a postprocessing refinement in order to smooth the jagged curves generated from the discretized domain and to achieve manufacturability [150]. As with the use of Cellular Materials, the main efforts of Topology Optimization processes have been focused in reducing mass while maximizing stiffness [151–154]. Then, the basic process shown in Figure 2b is hereafter termed as Topology Optimization Resulting in Cellular Patterns (TORCP).

There are other processes that combine Topology Optimization and Cellular Materials concepts in order to achieve specific stiffness values. For instance, Topology Optimization can be adopted to guide the material distribution and final configuration of unit cells in Cellular Materials. After the optimized unit-cell is obtained, a process to obtain the properties of the macromaterial in terms of the effective properties of its unit cell, termed as homogenization [155], is applied to approximate the apparent properties of the Cellular Material [146,156]. This widely used methodology is termed here as Topology Optimization Applied to Unit Cells (TOAUC), and it is graphically explained in Figure 9. The first implementation of Topology Optimization applied to unit-cell design can be found in the works of Sigmund [151,157,158]. Most recently, Osanov and Guest [159] reviewed the key requirements to apply topology optimization process to generate unit cells of periodic structured materials for a variety of customizable properties. Topology Optimization applied to the unit-cells of Cellular Materials has been used to maximize stiffness under general conditions [160–162], shear forces [163], and predetermined loads [164,165]. Resulting structures from 3D maximization stiffness problems are commonly closed-cell cellular structures [159,166]. This type of structure is preferred because their wall elements spans and connects various faces of the unit-cell, carrying loads axially in more than one direction, thus exhibiting stretch behavior in all directions. However, an important disadvantage of closed-cell structures with located enclosed pores is that they are quite difficult to fabricated. Furthermore, TOAUC-resulting cellular materials have been used to match specific stiffness values in bone implants [167–170].

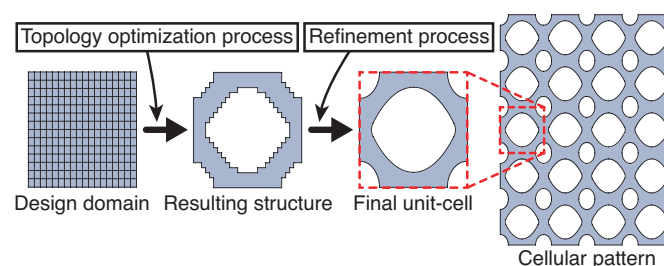


Figure 9. Process to tailor stiffness using Topology Optimization applied to the unit cells of Cellular Materials.

The maximization of stiffness by combination of the Topology Optimization and Cellular Materials techniques has also been explored. Two main concurrent methodologies were identified: The first begins with the typical Topology Optimization process to generate a conceptual design in the design domain. After that, the generated design is filled with a cellular structure especially selected to improve the optimization of the objective property. This concurrent method is termed here as Multiscale Topology Optimization with Cellular Materials (MTOCM), and it is graphically explained in Figure 10. Examples of relevant works using MTOCM approach can be found in [171–175].

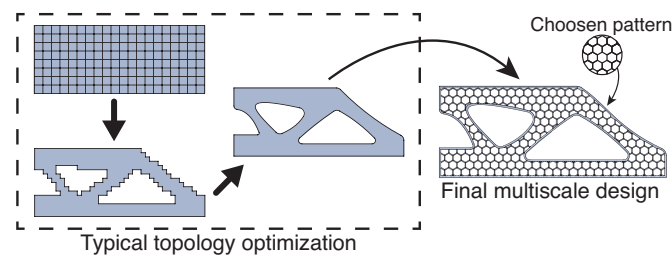


Figure 10. Process to tailor stiffness using the multiscale process that combines Topology Optimization with Cellular Materials.

The second concurrent methodology consists in modifying the relative density of the cellular design domain based on a Topology Optimization process, obtaining the so-called functionally graded Cellular Materials. Modification of the unit-cell relative density can be made by altering cell parameters [176] or by using different unit-cell topologies [177]. This methodology is termed as Topology Optimization of Functionally-graded Cellular Materials (TOFCM), and it is graphically explained in Figure 11. Other, examples of relevant works using TOFCM approach can be found in [178–182].

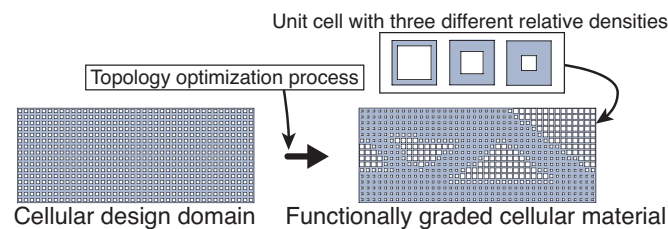


Figure 11. Process to tailor stiffness using Topology Optimization applied to cellular design domains that leads to functionally graded Cellular Materials.

Topology Optimization for tailoring stiffness with compliance objectives has been used to create compliant mechanisms [53], including micro-grippers [183], bridge-mechanisms [184], positioning stages [185], and path generating mechanisms [186]. However, using the Topology Optimization process to generate complete compliant mechanisms may lead to complex designs with distributed compliance throughout its topology, thus leading to complicated analysis, manufacturability, and further implementation [187]. Therefore, a new approach of Topology Optimization appeared as an alternative to deal with these drawbacks, maintaining the versatility of the process. This new approach is focused on applying the Topology Optimization process only on the flexures of compliant systems, taking the flexure section as the design domain of the Topology Optimization process. This could enhance the analysis of compliant systems through a proper characterization of their force deflection functions while maintaining their original macro-shape and lumped architecture.

In this regard, TORCP and TOAUC approaches are the most commonly employed when compliance is the goal property while applying Topology Optimization. They have been used to create cellular structures that are optimal in morphing applications [188–191], as well as in energy absorption applications [192–194]. Obtaining comparable levels of stiffness reductions and topologies with similar behaviors as the reported in Section 2. Moreover, the TOAUC method has been applied to create 2D [195–197] and 3D [198] extreme elastic materials that possess interesting properties such as a negative Poisson's ratio. The same process was used by Deng et al. [199] to create stretchable lattices with architected unit cells based on Bezier curves.

Topology Optimization in Compliant Systems as Flexure Elements

With the potential of Topology Optimization to design compliance materials already being stated, the works using this approach in compliance systems at flexure level are reviewed. For example, Topology Optimization has been used to design optimal compliant kinematic limbs that are part of larger compliant mechanisms [200–202]. A schematic

description of this process applied to the limbs of 2D flexure-based compliant parallel mechanisms is shown in Figure 12. Lum et al. [200] performed a Topology Optimization process to synthesize and optimize the topology, shape, and size of the limbs in a flexure-based compliant parallel mechanism (see Figure 12a), resulting in a significant improvement in the mechanism's workspace dimensions and increments in the mechanism's stiffness ratios, i.e., ratios of off-axis to actuating stiffness. Another work that dealt with the optimization of compliant kinematic limbs was that of Jin et al. [201], where those of 2D compliant parallel mechanisms were regarded as separate design domains for a Topology Optimization problems (see Figure 12(b-i,c-i)), and the Jacobian matrix was introduced into the field of Topology Optimization. This resulted in compliant parallel mechanisms with maximized workspaces that have compliant kinematic limbs accurately characterized facilitating the mechanism analysis. Later, Jin et al. [202] enhanced their previous research by including an improved stiffness evaluation generating new optimal compliant limbs and thus compliant parallel mechanisms (see Figure 12(b-ii,c-ii)) that have better levels of off-axis stiffness, and are similar to the generated in their previous work. Most recently, a different technique, not applied at the flexure level, has been used to design the limbs of compliant parallel platforms; this is based on keeping the mobile and fixed platforms as rigid bodies while applying a Topology Optimization process on a design domain that connects both platforms, examples using this technique designing 2D and 3D compliant parallel platforms can be found in [203–206], respectively.

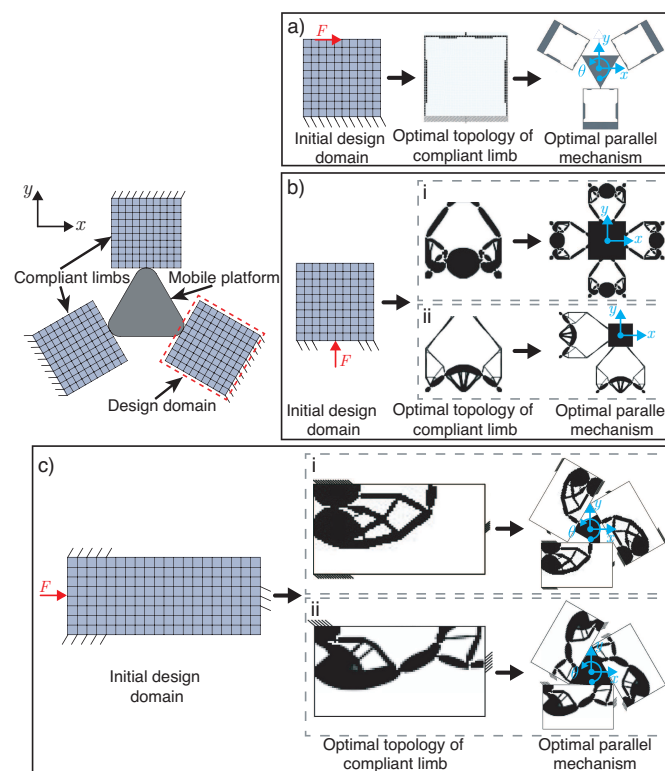


Figure 12. Schematic description of the Topology Optimization process to design the optimal compliant limbs of 2D compliant parallel mechanisms: (a) 3-DoF (x, y, θ) compliant parallel mechanism proposed by Lum et al. [200] (Adapted from [200] 2015, Elsevier); subfigures (b,c) are the 2-DoF (x, y) and the 3-DoF (x, y, θ) compliant parallel mechanisms, respectively, proposed by Jin et al. found in (i) [201] (Adapted from [201] 2016, Elsevier); and (ii) [202] (Adapted from [202] 2018, ASME).

Topology Optimization of single flexures, i.e., those that are not part of a compliant mechanism, has been also addressed. The most commonly studied single flexures are the Single-Axis Rotational Flexure Joints (SARFJ). Studies of Topology Optimization used in the design of SARFJ can be categorized according to the geometry of the design

domain used in the process. Initial attempts were performed using 2D rectangular design domains as shown in Figure 13. Examples using this approach are the works of Zhu et al. [207–209]. In [207], Zhu et al. performed the design and optimization of SARFJ, searching to maximize the compliance in the desired direction while minimizing the compliance in the other directions. The design problem was modeled and analyzed as a small-displacement problem using linear Finite Element Analysis (FEA) resulting in the final design shown in Figure 13a. Compared with the constant rectangular cross section flexure hinge of similar mass, the optimized design showed more compliance, capable of undergoing a larger rotation angle when subjected to the same external load, while achieving rotation with better precision. However, the obtained design reaches higher levels of stress. Then, in [208], the same authors extended their previous work by including “fixing the coordinates of the rotational center O ” as an additional objective in the Topology Optimization problem. This additional objective was attempted by setting the topology to be symmetric with respect to x - and y -axes in the design domain resulting in the topology shown in Figure 13b. However, the resulting design showed lower precision than their previous design, demonstrating that minimizing the displacement of the point O must be added as a constraint in the Topology Optimization problem instead of an objective. Most recently, Zhu et al. [209] improved their work in [207] by maintaining the functional requirements of maximizing the compliance in the desired direction, while minimizing the compliance in the other directions and setting “minimizing the displacement of the rotational center O ” and symmetry of the topology in both axes, as constraints of the process. The resulting design was similar to that of the cartwheel flexure joint (see Figure 13c), often regarded as a flexure joint with ultra-high rotation accuracy. Additional designs were created by changing the allowable material usage and the geometry of the design domain. In general, the resulting topologies showed great rotational precision and high levels of compliance in the motion direction.

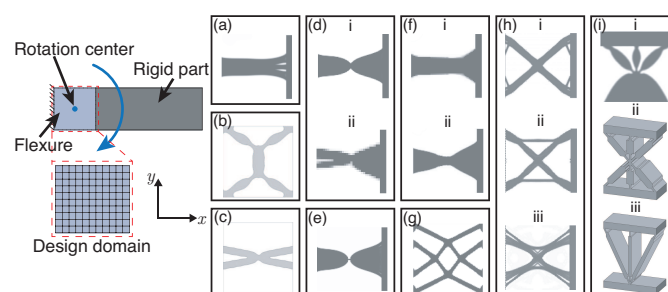


Figure 13. Schematic description of the Topology Optimization process to design the optimal configuration of SARFJ using a 2D rectangular design domain. Optimal designs were obtained in (and adapted from) (a) [207]; (b) [208]; (c) [209]; (d) [210] i-design based on linear FEA and ii-design based on nonlinear FEA; (e) [211]; (f) [212] i-design with less stress allowed for a mesh of 50×50 and ii-design with less stress allowed for a mesh of 100×100 ; (g) [213]; (h) [214] i-design for general distributed flexure hinges, ii-design for distributed flexure hinges with prescribed compliances, and iii-design for distributed flexure hinges with minimal parasitic motion; and (i) [56] i-optimal topology, ii-simplified design named “Snowflake”, and iii-simplified design named “Half-Snowflake”.

The Topology Optimization of SARFJ, using a 2D rectangular design domain, was addressed also by Liu et al. [210–214]. In [210], the authors dealt with the Topology Optimization of SARFJ undergoing large displacement by using a geometrically nonlinear elastic analysis in the Topology Optimization process. The optimization problem was formulated to set the stiffness of the flexure joint at the functional direction as low as possible and the stiffness at non-functional direction as high as possible. Additionally, minimizing the displacement of the center of rotation point and symmetry about x -axis were added as constraints. Two optimal designs were created: one based on linear FEA (see Figure 13(d-i) and other using nonlinear FEA (see Figure 13(d-ii). The resulting designs were compared with a filleted V-shape flexure hinge. Results showed

that nonlinear design can reach the highest rotation angle and has the lowest level of stress concentration. On the other hand, the linear design has better precision but the highest level of stress. This was further extended in [211], with the design of a three-segment flexure joint named quasi-V-shaped flexure hinge (QVFH) shown in Figure 13e. The authors derived the in-plane compliance equations for small displacements based on Castigliano's second theorem. Compared with the filleted V-shaped flexure hinge, the QVFH showed less compliance, more precision in keeping the center of rotation with the minimal offset, and larger maximum stress level. After that, Liu et al. [212] designed flexure joints by using stress-constrained Topology Optimization, aiming to reduce the general stress level and remove the sharp corners of the flexure hinges, thereby reducing the stress concentration and improving the range of motion. Various topologies were created for several levels of stress limit. The resulting final topology without stress constraint is similar to the one obtained in [211]. It can be observed that when the stress constraints are added, the length and thickness of the middle segment become longer and thicker, respectively, thus removing sharp corners distributing the stress and reducing stress concentrations. Several designs were created varying the level of stress constraint and changing the mesh refinement of the design domain, only two final topologies are shown in Figure 13f, corresponding to the designs with less stress allowed for a mesh of 50×50 (see Figure 13(f-i)) and for a mesh of 100×100 (see Figure 13(f-ii)). As it can be seen, optimal designs with stress constraints tend to seem blade flexures, therefore losing precision.

In this regard, Liu et al. [213] presented a systematic method for designing flexure hinges with distributed stress by using Topology Optimization with the objective of maximizing the bending displacement while minimizing the axial displacement and at the same time to minimize the maximum level of stress. Additionally, a symmetry constraint in both x - and y -axes was added, resulting in the non-conventional notch flexure hinge, shown in Figure 13g, that exhibited distributed stress. Finally, this work was extended in [214], where authors designed flexure hinges with a symmetrical distributed configuration that accomplish the desired performances of prescribed compliance and minimal parasitic motion. Several designs were obtained for each desired performance; only three of them are shown in Figure 13h, accounting for general distributed flexure hinges (see Figure 13(h-i)), distributed flexure hinges with prescribed compliances (see Figure 13(h-ii)), and distributed flexure hinges with minimal parasitic motion (see Figure 13(h-iii)). Resulting configurations are similar to the cartwheel flexure hinge which, as was mentioned before, it is well known for being a high precision flexure joint. Finally, Pinskiar et al. [56] used Topology Optimization to design SARFJ to account for the goals of motion-range, compliance, and precision simultaneously. The resulting main topology is shown in Figure 13(i-i). Based on this topology, a second design stage was performed to produce two simplified hinge designs named "Snowflake" and "Half-Snowflake" shown in Figure 13(i-ii,iii), respectively. After comparing their performance, the new type of flexure hinge showed higher precision and comparable levels of rotational compliance than blade and cross-axis flexures. Additionally, the resulting structures have extra members that could lead to an off-axis stiffness increment, reducing parasitic displacements and making them able to transfer forces.

Other optimal designs of SARFJ were created using 2D design domains, based on the geometry of a right circular flexure hinge as shown in Figure 14. For instance, Liu et al. [215] used Topology Optimization to remove material from a right circular flexure hinge in order to increase compliance while retaining high precision, resulting in the multi-notched flexure hinge topology shown in Figure 14(a-i). Several topologies were obtained using different dimensions in the design domain and varying the percentage of removed material; however, they resulted in nearly the same for all examples. Then, a final shape of the multi-notched flexure hinge (see Figure 14(a-ii)) was proposed after a postprocessing refinement stage and was used for comparison in its performance with various flexure hinges (right circular [216], corner-filleted [217], elliptical [218], parabolic, and hyperbolic [219]). Results showed that the multi-notched flexure hinges can have larger rotational compliance, higher rotational precision, and lower stress levels than any other type of flexure hinge when certain dimensional conditions are satisfied. Additionally, Zhu et al. [209] obtained

a similar topology, shown in Figure 14b, using Topology Optimization with a multi-criteria objective function and a symmetry constraint. The resulting design showed great rotational precision and high levels of compliance in the motion direction.

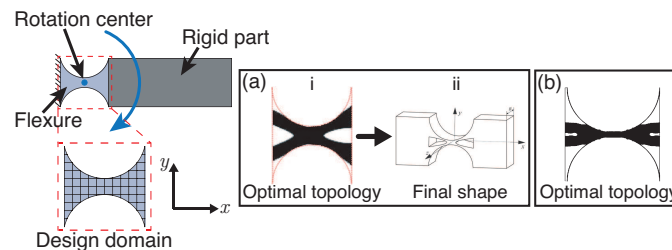


Figure 14. Schematic description of the Topology Optimization process to design the optimal configuration of SARFJ using a 2D design domain based on the geometry of a right circular flexure hinge. Optimal designs obtained: (a) i-optimal topology and ii-final shape (Adapted with permission from ref. [215]. 2021, Elsevier) and (b) optimal topology obtained in [209] (Adapted from ref. [209]. 2019, Springer).

Most recently, 3D design domains were also used in Topology Optimization to generate SARFJ as shown in Figure 15. Qiu et al. [220] used 3D continuum Topology Optimization to find the optimal topology of a SARFJ in a 3D design domain. The resulting topology is the single-axis multi-cavity flexure hinge (MCFH) shown in Figure 15(a-i). After that, a postprocessing stage was used to simplify the configuration of the hinge resulting in the final design shown in Figure 15(a-ii). Dimensionless empirical equations of the stiffness performance were obtained based on FEA for this simplified MCFH. Then, the new flexure hinge was compared with other types of hinges demonstrating that the MCFH have greater compliance. Then, Qiu et al. [221] presented a dual-objective Topology Optimization process for maximization of compliance and precision performance of flexure hinges based on 3D continuum Topology Optimization. The resulting topology, shown in Figure 15(b-i), was further postprocessed and parameterized generating the single-axis quasi-leaf porous flexure hinge (QLPFH) shown in Figure 15(b-ii). Dimensionless empirical equations of the stiffness and rotational center performance were derived with the aid of FEA, and they were used for comparison with a leaf flexure hinge with the same envelope space dimensions. The results showed that the rotational compliance of QLPFH is much larger than of the leaf flexure. In addition, the precision performance of the QLPFH was also improved significantly.

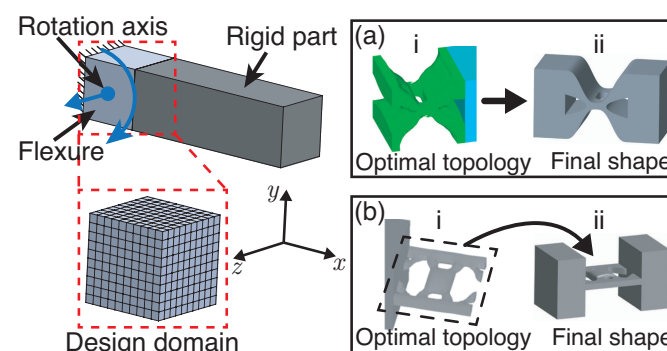


Figure 15. Schematic description of the Topology Optimization process to design the optimal configuration of SARFJ using a 3D cubic design domain. Optimal designs obtained in (a) i-optimal topology and ii-final shape (Adapted with permission from ref. [220]. 2021, Elsevier), (b) i-optimal topology and ii-final shape (Adapted from ref. [221]. 2020, Springer).

Topology Optimization has also been used to find the optimal material distribution in a less common type of flexure joint called “compliant revolute joint” (Figure 16). The compliant revolute joint consists of a thin cylinder of compliant material with a inner hollow where

its external face is fixed and its internal face is subject to a rotational displacement produced by a tangential force applied at the same face. Li et al. [222–224] presented a series of works dealing with the Topology Optimization of this type of flexure joint. In [222], the authors designed new compliant revolute joints reconstructed after removing material with a Topology Optimization process. The obtained designs are shown in Figure 16(i–iv). FEA was used to compare the performance of the optimized designs with the non-optimized compliant revolute joint. Results showed that optimized designs can achieve more rotational displacement. However, their stress levels were also increased. Further experimental validation in the rotational angle and stress levels of the optimal designs was performed in [223], obtaining a maximum error between experimental and FEA results of 8.7%. This was expanded in [224], by modeling the compliant revolute joint as a kinetoelastic model considering the kinematic properties and structural elastic properties simultaneously. This approach allowed obtaining optimized compliant revolute joints with desirable compliance properties that are quite similar to those obtained in their previous works.

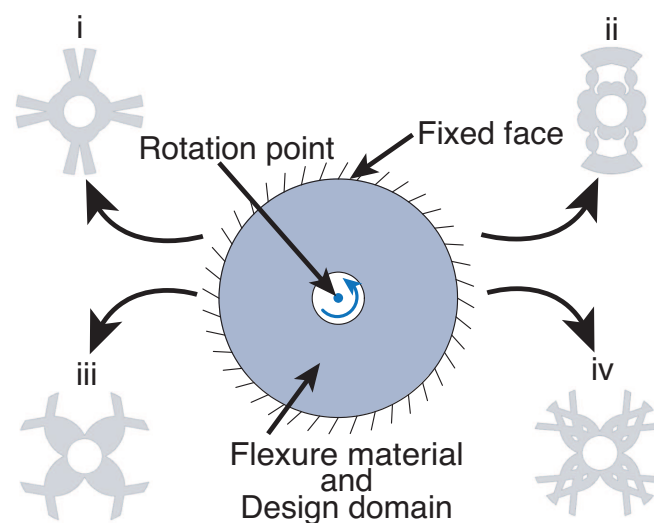


Figure 16. Schematic description of the Topology Optimization process to design the optimal configuration of SARFJ using a 2D design domain based on the geometry of compliant revolute joint. (i–iv) Optimal designs obtained in [222] (Adapted from ref. [222]. 2017, Springer).

Furthermore, Topology Optimization has been used to achieve the optimal material distribution of single-axis translational flexure joints (SATFJ) based on the geometry of blade flexures (see Figure 17). Pinskiar et al. [2,52] investigated the design of this type of flexure to be used in parallelogram linear flexure guides using Topology Optimization to maximize their ratio of in-plane to out-of-plane stiffness. The resulting topology shown in Figure 17(a-i) resembles a X-type lattice structure similar to that used in [22] (see Figure 8). After that, a parameterized flexure design was generated based on the resulting topology (see Figure 17(a-ii)), and it showed stiffness ratios of 1.5 to 6 times greater than standard blade structures with mass reductions up to 75%.

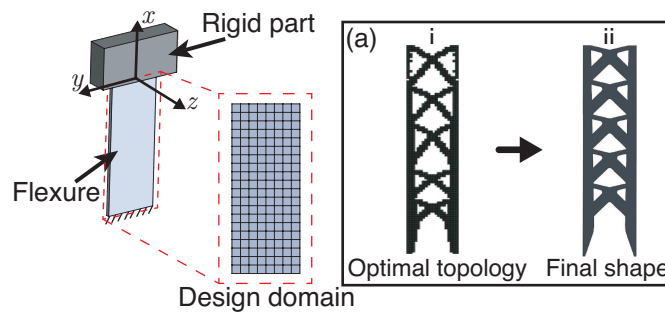


Figure 17. Schematic description of the Topology Optimization process to design the optimal configuration of SATFJ using a 2D design domain based on the geometry of blade flexures. (a) Optimal design obtained in [52] i-optimal topology and ii-final shape (reprinted with permission from [52], 2019, Elsevier).

4. Remarks on Tailoring Stiffness via Cellular Materials and Topology Optimization

Cellular Materials and Topology Optimization can be used effectively for tailoring stiffness. The Cellular Materials approach is based on the proper selection of the unit-cell that constructs the cellular material; note that this approach works on the micro-scale. On the other hand, the Topology Optimization approach generates an optimal topology for specific external load conditions; then, it is said that this approach acts on the macro-scale. Therefore, both approaches can be combined to take advantage of their particular characteristics at the same time. A summary that address advantages and disadvantages of Cellular Materials and Topology Optimization approaches as well as their combinations, is presented in the diagram in Figure 18.

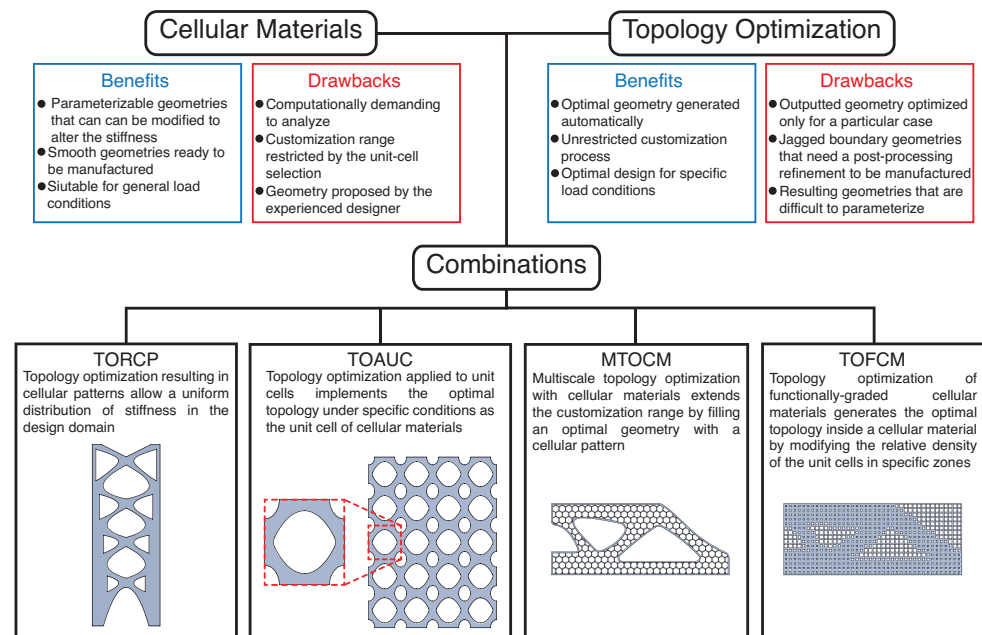


Figure 18. Summary diagram of the Cellular Materials and Topology Optimization approaches and their combinations.

In addition, the implementation of Cellular Materials and Topology Optimization approaches for tailoring stiffness in compliant systems entails the modification of other mechanical characteristics such as weight reduction, stiffness ratios, stress relief, and motion range. Therefore, a brief discussion on how these characteristics are modified as the stiffness is modified is presented here.

Weight reduction

Stiffness reduction via Cellular Materials and Topology Optimization approaches implies removing material. Therefore, a reduction in stiffness brings with it a weight

reduction. The key aspect relies on a controlled removing of material (or distribution of material), so that this reduction in overall weight can be related to the resulting mechanical properties. A random removal of material will in turn reduce stiffness and weight; however, the control of the resulting mechanics becomes a trail and error process (non-systematic).

Motion range

The motion range of a compliant system is related to the elastic displacement. This scales with the elastic modulus of the structure, i.e., its stiffness. Therefore, any attempt to tailor the stiffness of the cellular material or optimize the topology will lead to modifications in the motion range that can be achieved. Another aspect that can come with the incorporation of any of the two approaches is the anisotropy, as the proposed or resulting geometries may be directionally dependent. Structures made of anisotropic materials can have displacements in directions apart from the those aligned to the loading axis.

Stress relief

The use of Cellular Materials and Topology Optimization approaches for stiffness reduction often leads to geometries with sharp corners, thus incrementing the stress level. However, by controlling the topology of a cellular material, it is possible to tune the localization and magnitude of the stress [100] in a structure. Moreover, certain cellular structures such as the contact-aided patterns have been used to provide stress relief [44–46], while others such as the auxetic patterns allow a better stress distribution due to their high flexibility [119].

Stiffness ratios

Stiffness ratios allow one to compare the stiffness levels in different directions. A flexure element commonly needs great flexibility in certain directions while maintaining high levels of stiffness in the others, i.e., its stiffness ratios must be large. The use of Cellular Materials and Topology Optimization approaches for stiffness reduction in certain direction generally produce stiffness reductions also in the others. However, the stiffness reduction in the desired direction is significantly higher than in the non-desired directions, thus incrementing the stiffness ratios [22]. Moreover, the stiffness ratios can be maximized in the Topology Optimization process [52].

5. Conclusions

Cellular Materials and Topology Optimization can be considered as approaches to tailor properties by selectively removing material, e.g., stiffness, in a structure eliminating the need of additional elements and maintaining the overall dimensions of the piece. These approaches appear as a possible solution to deal with inaccuracies and limitations of compliant systems. In this work, these two were reviewed regarding their used in tailoring the stiffness of flexure elements. Interest in both has grown in recent years due to the increasing availability of additive manufacturing processes. These allow the fabrication of complex geometries with a controlled distribution of matter, comparable to the ones resulting from these approaches. It was then relevant to overview both approaches, so that the users and readers can compare and contrast prior selecting one of them.

Regarding Cellular Materials, stretch-dominated structures are preferred when maximizing stiffness is the objective, while bending-dominated structures are the best option for compliance applications. Two-dimensional bending-dominated lattice arrangements have been more frequently used in compliance applications. The use of bending-dominated 3D closed-cell structures has been studied recently in energy absorption applications, demonstrating their capacity to be used for compliance purposes. Therefore, tailoring stiffness of flexures via Cellular Materials using 3D and closed-cell structures appears to be a promising option, due to the design advantages such as high off-axis stiffness and greater load bearing capacity.

Auxetic architectures are the most widely used in compliance applications because of their high deformations under relatively low stresses. However, the use of these type of architectures in flexure elements has not been explored. In addition, cellular structures with a zero-Poisson ratio represent another type of non-explored architecture. This type of metastructure is characterized for providing deformation in one direction while maintaining unchanged its dimensions in the others. This particular deformation-mechanism could

be useful in the design of flexure elements and compliant mechanisms to avoid parasitic motions due to non-desire displacements.

Numerous literature has focused on flexure joints for rotational motion, while very few works on joints for other types of motion were encountered. Research has been focused almost entirely on SARFJ leaving unexplored other types of joints such as prismatic or cylindrical. The wide variety of Cellular Materials may allow the creation of unexplored compliant joints that commonly need more than one flexure to be conformed.

On the other hand, the use of Topology Optimization allows finding the best option of material distribution, and with the use of computational power, this could be done relatively fast. However, it often leads to a complex architecture that requires a postprocessing stage to obtain the final design. Furthermore, the resulting design could be difficult to parametrize and handle analytically, compromising the prediction of the behavior under any other conditions different from the ones used in formulation of the optimization process. As opposed to this, the use of Cellular Materials allows an accurate structure-property relation. Still, the potential tailorability is limited to the Cellular Material topologies. Therefore, combinations of Cellular Materials and Topology Optimization, i.e., TOAUC, MTOCM, and TOFCM, must be explored in the design of flexure elements making use of the advantages offered by both approaches.

The use of Topology Optimization in the design of flexure joints has been studied more than that of Cellular Materials. Looking at the evolution of the Topology Optimization of flexure joints, it is possible to see that the tendency is to create designs with distributed compliance through the implementation of repeatable members in their geometrical space, avoiding the concentration of deformation in a single element. Therefore, Topology Optimization can be used as a first stage in the design of flexure elements, after that it can be followed by adjusting the material distribution by means of Cellular Material topology, therefore having a controlled structure-property relation and perhaps a simplification of the design.

Finally, further trends in research in this area and recommendations to extend the study of tailoring stiffness of flexure elements via Cellular Materials and Topology Optimization are provided based on the available literature reviewed here.

1. Due to their advantages in tailoring the mechanical properties, exploring the use of closed-cell structures, 3D arrays, auxetic, and zero-Poisson architectures in tailoring the stiffness of flexure elements could lead to benefits compliant systems.
2. As flexures base their functioning on the elastic response of their elements, other material properties, i.e., Poisson's ratio, could complicate their use to build up other kinematic pairs, e.g., cylindrical. However, a correct selection of cellular pattern could be designed so that it restricts the Poisson's ratio to 0. This opens up a new range of possibilities in compliant systems applications.
3. Combining both Cellular Materials and Topology Optimization approaches (TOAUC, MTOCM, and TOFCM) to expand the possibilities in tailoring stiffness of flexure elements. This combination leads to obtain the best out of each. An example of the use of these two could be by implementing Topology Optimization at the conceptual design stage for the proposal of a flexure element. Then, employ a Cellular Material to adjust the stiffness by modifying the parameters that define the structure.
4. Analytical parameterization of the Cellular Material employed can result in an accurate and precise tracking of the stiffness. This allows a controlled tailoring of stiffness in compliant systems.
5. Another aspect to keep in mind is that lattice honeycombs might have in-plane anisotropy. Therefore, when used in flexures, the proper selection of orientation becomes crucial. Failure in considering this could lead to deformations in non-desired directions, i.e., parasitic motions.

Author Contributions: Conceptualization, M.A.-S. and E.C.-U.; methodology, M.A.-S., E.C.-U., and A.G.-E.; investigation, M.A.-S.; writing—original draft preparation, M.A.-S.; writing—review and editing, E.C.-U. and A.G.-E.; supervision, E.C.-U. and A.G.-E.; project administration, A.G.-E. All authors have read and agreed to the published version of the manuscript.

Funding: The authors would like to acknowledge the financial support of Tecnológico de Monterrey, in the production of this work.

Acknowledgments: The authors would like to acknowledge support from CONACyT for PhD studies of first author (scholarship number 863078) and nTopology for providing access to research and academic licenses.

Conflicts of Interest: The authors declare no conflicts of interest.

Abbreviations

MEMS	Microelectromechanical Systems
3D	Three-dimensional
DOF	Degrees of Freedom
2D	Two-dimensional
SIMP	Solid Isotropic Material with Penalization
TORCP	Topology Optimization Resulting in Cellular Patterns
TOAUC	Topology Optimization Applied to Unit Cells
MTOCM	Multiscale Topology Optimization with Cellular Materials
TOFCM	Topology Optimization of Functionally-graded Cellular Materials
SARFJ	Single Axis Rotational Flexure Joints
FEA	Finite Element Analysis
QVFH	Quasi V-shaped Flexure Hinge
MCFH	Multi-Cavity Flexure Hinge
QLPFH	Quasi-Leaf Porous Flexure Hinge
SATFJ	Single-Axis Translational Flexure Joints

References

- Howell, L.L. *Compliant Mechanisms*; Wiley: New York, NY, USA, 2001.
- Pinskiar, J.; Shirinzadeh, B. Topology optimization of leaf flexures for stiffness ratio maximization in compliant mechanisms. In Proceedings of the 2018 IEEE/ASME International Conference on Advanced Intelligent Mechatronics (AIM), Auckland, New Zealand, 9–12 July 2018; IEEE: Piscataway, NJ, USA, 2018; pp. 407–412. [[CrossRef](#)]
- Tian, Y.; Zhang, D.; Shirinzadeh, B. Dynamic modelling of a flexure-based mechanism for ultra-precision grinding operation. *Precis. Eng.* **2011**, *35*, 554–565. [[CrossRef](#)]
- Cecchi, R.; Verotti, M.; Capata, R.; Dochshanov, A.; Broggiato, G.B.; Crescenzi, R.; Balucani, M.; Natali, S.; Razzano, G.; Lucchese, F.; et al. Development of micro-grippers for tissue and cell manipulation with direct morphological comparison. *Micromachines* **2015**, *6*, 1710–1728. [[CrossRef](#)]
- Zubir, M.N.M.; Shirinzadeh, B.; Tian, Y. Development of a novel flexure-based microgripper for high precision micro-object manipulation. *Sensors Actuators A Phys.* **2009**, *150*, 257–266. [[CrossRef](#)]
- Fleming, A.J.; Yong, Y.K. An ultrathin monolithic XY nanopositioning stage constructed from a single sheet of piezoelectric material. *IEEE/ASME Trans. Mechatron.* **2017**, *22*, 2611–2618. [[CrossRef](#)]
- Kota, S.; Joo, J.; Li, Z.; Rodgers, S.M.; Sniegowski, J. Design of compliant mechanisms: Applications to MEMS. *Analog. Integr. Circuits Signal Process.* **2001**, *29*, 7–15. [[CrossRef](#)]
- Sun, X.; Yang, B. A new methodology for developing flexure-hinged displacement amplifiers with micro-vibration suppression for a giant magnetostrictive micro drive system. *Sens. Actuators A Phys.* **2017**, *263*, 30–43. [[CrossRef](#)]
- Chen, B.K.; Zhang, Y.; Sun, Y. Active release of microobjects using a MEMS microgripper to overcome adhesion forces. *J. Microelectromech. Syst.* **2009**, *18*, 652–659. [[CrossRef](#)]
- Ling, M.; Howell, L.L.; Cao, J.; Chen, G. Kinetostatic and dynamic modeling of flexure-based compliant mechanisms: A survey. *Appl. Mech. Rev.* **2020**, *72*, 030802. [[CrossRef](#)]
- Lee, C.; Stepanick, C.K.; Lee, S.K.; Tarbuton, J.A. Cross-coupling effect of large range XY nanopositioning stage fabricated by stereolithography process. *Precis. Eng.* **2016**, *46*, 81–87. [[CrossRef](#)]
- Yuanqiang, L.; Wangyu, L. Analysis of the displacement of distributed compliant parallel-guiding mechanism considering parasitic rotation and deflection on the guiding plate. *Mech. Mach. Theory* **2014**, *80*, 151–165. [[CrossRef](#)]
- Luo, Y.; Liu, W.; Wu, L. Analysis of the displacement of lumped compliant parallel-guiding mechanism considering parasitic rotation and deflection on the guiding plate and rigid beams. *Mech. Mach. Theory* **2015**, *91*, 50–68. [[CrossRef](#)]
- Cornelissen, R.; Müller, A.; Aarts, R. A Compliant and Redundantly Actuated 2-DOF 3RRR PKM: Best of Both Worlds? In Proceedings of the IFToMM World Congress on Mechanism and Machine Science, Duisburg, Germany, 26 August 2019; Springer: Berlin/Heidelberg, Germany, 2019; pp. 163–171. [[CrossRef](#)]

15. Yun, Y.; Li, Y. Design and analysis of a novel 6-DOF redundant actuated parallel robot with compliant hinges for high precision positioning. *Nonlinear Dyn.* **2010**, *61*, 829–845. [[CrossRef](#)]
16. Merriam, E.G.; Lund, J.M.; Howell, L.L. Compound joints: Behavior and benefits of flexure arrays. *Precis. Eng.* **2016**, *45*, 79–89. [[CrossRef](#)]
17. Li, S.; Yu, J. Design principle of high-precision flexure mechanisms based on parasitic-motion compensation. *Chin. J. Mech. Eng.* **2014**, *27*, 663–672. [[CrossRef](#)]
18. Yong, Y.K.; Liu, K.; Moheimani, S.R. Reducing cross-coupling in a compliant XY nanopositioner for fast and accurate raster scanning. *IEEE Trans. Control. Syst. Technol.* **2009**, *18*, 1172–1179. [[CrossRef](#)]
19. Zhang, Z.; Yang, X.; Yan, P. Large dynamic range tracking of an XY compliant nanomanipulator with cross-axis coupling reduction. *Mech. Syst. Signal Process.* **2019**, *117*, 757–770. [[CrossRef](#)]
20. Bhagat, U.; Shirinzadeh, B.; Tian, Y.; Zhang, D. Experimental analysis of laser interferometry-based robust motion tracking control of a flexure-based mechanism. *IEEE Trans. Autom. Sci. Eng.* **2012**, *10*, 267–275. [[CrossRef](#)]
21. Liu, Z.; Zhang, Z.; Yan, P. A Spatial Design of a Large Stroke Compliant XY Nanomanipulator with Cross-Coupling Error Reduction. In Proceedings of the 2019 International Conference on Manipulation, Automation and Robotics at Small Scales (MARSS), Helsinki, Finland, 1–5 July 2019; IEEE: Piscataway, NJ, USA, 2019; pp. 1–6. [[CrossRef](#)]
22. Merriam, E.G.; Howell, L.L. Lattice flexures: Geometries for stiffness reduction of blade flexures. *Precis. Eng.* **2016**, *45*, 160–167. [[CrossRef](#)]
23. Ham, R.V.; Sugar, T.; Vanderborght, B.; Hollander, K.; Lefeber, D. Compliant actuator designs. *IEEE Robot. Autom. Mag.* **2009**, *3*, 81–94. [[CrossRef](#)]
24. Vanderborght, B.; Albu-Schäffer, A.; Bicchi, A.; Burdet, E.; Caldwell, D.G.; Carloni, R.; Catalano, M.; Eiberger, O.; Friedl, W.; Ganesh, G.; et al. Variable impedance actuators: A review. *Robot. Auton. Syst.* **2013**, *61*, 1601–1614. [[CrossRef](#)]
25. Pluimers, P.J.; Tolou, N.; Jensen, B.D.; Howell, L.L.; Herder, J.L. A compliant on/off connection mechanism for preloading statically balanced compliant mechanisms. In Proceedings of the International Design Engineering Technical Conferences and Computers and Information in Engineering Conference, Chicago, IL, USA, 12–15 August 2012; American Society of Mechanical Engineers (ASME): New York, NY, USA, 2012; Volume 4, pp. 373–377. [[CrossRef](#)]
26. Stapel, A.; Herder, J.L. Feasibility study of a fully compliant statically balanced laparoscopic grasper. In Proceedings of the International Design Engineering Technical Conferences and Computers and Information in Engineering Conference, Salt Lake City, UT, USA, 28 September–2 October 2004; Volume 2, pp. 635–643. [[CrossRef](#)]
27. Merriam, E.G.; Howell, L.L. Non-dimensional approach for static balancing of rotational flexures. *Mech. Mach. Theory* **2015**, *84*, 90–98. [[CrossRef](#)]
28. Chen, G.; Zhang, S. Fully-compliant statically-balanced mechanisms without prestressing assembly: Concepts and case studies. *Mech. Sci.* **2011**, *2*, 169–174. doi:10.5194/ms-2-169-2011. [[CrossRef](#)]
29. Dunning, A.; Tolou, N.; Herder, J. A compact low-stiffness six degrees of freedom compliant precision stage. *Precis. Eng.* **2013**, *37*, 380–388. [[CrossRef](#)]
30. Morsch, F.M.; Herder, J.L. Design of a generic zero stiffness compliant joint. In Proceedings of the International Design Engineering Technical Conferences and Computers and Information in Engineering Conference, Montreal, QC, Canada, 15–18 August 2010; Volume 2, pp. 427–435. [[CrossRef](#)]
31. Schiavi, R.; Grioli, G.; Sen, S.; Bicchi, A. VSA-II: A novel prototype of variable stiffness actuator for safe and performing robots interacting with humans. In Proceedings of the 2008 IEEE International Conference on Robotics and Automation, Pasadena, CA, USA, 19–23 May 2008; IEEE: Piscataway, NJ, USA, 2008; pp. 2171–2176. [[CrossRef](#)]
32. Liu, Y.; Liu, X.; Yuan, Z.; Liu, J. Design and analysis of spring parallel variable stiffness actuator based on antagonistic principle. *Mech. Mach. Theory* **2019**, *140*, 44–58. [[CrossRef](#)]
33. Jafari, A.; Tsagarakis, N.G.; Vanderborght, B.; Caldwell, D.G. A novel actuator with adjustable stiffness (AwAS). In Proceedings of the 2010 IEEE/RSJ International Conference on Intelligent Robots and Systems, Taipei, Taiwan, 18–22 October 2010; IEEE: Piscataway, NJ, USA, 2010; pp. 4201–4206. [[CrossRef](#)]
34. Jafari, A.; Tsagarakis, N.G.; Caldwell, D.G. AwAS-II: A new actuator with adjustable stiffness based on the novel principle of adaptable pivot point and variable lever ratio. In Proceedings of the 2011 IEEE International Conference on Robotics and Automation, Shanghai, China, 9–13 May 2011; IEEE: Piscataway, NJ, USA, 2011; pp. 4638–4643. [[CrossRef](#)]
35. Sun, J.; Guo, Z.; Sun, D.; He, S.; Xiao, X. Design, modeling and control of a novel compact, energy-efficient, and rotational serial variable stiffness actuator (SVSA-II). *Mech. Mach. Theory* **2018**, *130*, 123–136. [[CrossRef](#)]
36. Choi, J.; Hong, S.; Lee, W.; Kang, S.; Kim, M. A robot joint with variable stiffness using leaf springs. *IEEE Trans. Robot.* **2011**, *27*, 229–238. [[CrossRef](#)]
37. Wang, W.; Fu, X.; Li, Y.; Yun, C. Design of variable stiffness actuator based on modified Gear–Rack mechanism. *J. Mech. Robot.* **2016**, *8*, 061008. [[CrossRef](#)]
38. Hawks, J.C.; Colton, M.B.; Howell, L.L. A variable-stiffness straight-line compliant mechanism. In Proceedings of the International Design Engineering Technical Conferences and Computers and Information in Engineering Conference, Boston, MA, USA, 2–5 August 2015; American Society of Mechanical Engineers: New York, NY, USA, 2015; Volume 5A, p. V05AT08A011, [[CrossRef](#)]
39. Xie, Z.; Qiu, L.; Yang, D. Design and analysis of a variable stiffness inside-deployed lamina emergent joint. *Mech. Mach. Theory* **2018**, *120*, 166–177. [[CrossRef](#)]

40. Galloway, K.C.; Clark, J.E.; Koditschek, D.E. Variable stiffness legs for robust, efficient, and stable dynamic running. *J. Mech. Robot.* **2013**, *5*, 011009. [[CrossRef](#)]
41. Wissa, A.; Tummala, Y.; Hubbard, J., Jr.; Frecker, M.I. Passively morphing ornithopter wings constructed using a novel compliant spine: Design and testing. *Smart Mater. Struct.* **2012**, *21*, 094028. [[CrossRef](#)]
42. Tummala, Y.; Frecker, M.I.; Wissa, A.; Hubbard, J.E., Jr. Design and optimization of a bend-and-sweep compliant mechanism. *Smart Mater. Struct.* **2013**, *22*, 094019. [[CrossRef](#)]
43. Tummala, Y.; Wissa, A.; Frecker, M.; Hubbard, J.E. Design and optimization of a contact-aided compliant mechanism for passive bending. *J. Mech. Robot.* **2014**, *6*, 031013. [[CrossRef](#)]
44. Mehta, V.; Frecker, M.; Lesieutre, G.A. Stress relief in contact-aided compliant cellular mechanisms. *J. Mech. Des.* **2009**, *131*, 091009. [[CrossRef](#)]
45. Mankame, N.D.; Ananthasuresh, G. A novel compliant mechanism for converting reciprocating translation into enclosing curved paths. *J. Mech. Des.* **2004**, *126*, 667–672. [[CrossRef](#)]
46. Cannon, J.R.; Howell, L.L. A compliant contact-aided revolute joint. *Mech. Mach. Theory* **2005**, *40*, 1273–1293. [[CrossRef](#)]
47. Guérinot, A.E.; Magleby, S.P.; Howell, L.L.; Todd, R.H. Compliant joint design principles for high compressive load situations. *J. Mech. Des.* **2005**, *127*, 774–781. [[CrossRef](#)]
48. Gupta, G.; Tan, J.; Seepersad, C.C. ME Design and Freeform Fabrication of Compliant Cellular Materials with Graded Stiffness. In Proceedings of the 2006 International Solid Freeform Fabrication Symposium, Austin, TX, USA, 14–16 August 2006.
49. Jovanova, J.; Nastevska, A.; Frecker, M. Tailoring energy absorption with functional grading of a contact-aided compliant mechanism. *Smart Mater. Struct.* **2019**, *28*, 084003. [[CrossRef](#)]
50. Xie, Z.; Qiu, L.; Yang, D. Using the Parts Used to Be Removed to Improve Compliant Joint's Performance. In Proceedings of the International Design Engineering Technical Conferences and Computers and Information in Engineering Conference, Quebec City, QC, Canada, 26–29 August 2018; American Society of Mechanical Engineers: New York, NY, USA, 2018; Volume 5A, p. V05AT07A006. [[CrossRef](#)]
51. Xie, Z.; Qiu, L.; Yang, D. Analysis of a novel variable stiffness filleted leaf hinge. *Mech. Mach. Theory* **2020**, *144*, 103673. [[CrossRef](#)]
52. Pinskiér, J.; Shirinzadeh, B. Topology optimization of leaf flexures to maximize in-plane to out-of-plane compliance ratio. *Precis. Eng.* **2019**, *55*, 397–407. [[CrossRef](#)]
53. Zhu, B.; Zhang, X.; Zhang, H.; Liang, J.; Zang, H.; Li, H.; Wang, R. Design of compliant mechanisms using continuum topology optimization: A review. *Mech. Mach. Theory* **2020**, *143*, 103622. [[CrossRef](#)]
54. Gallego, J.A.; Herder, J. Synthesis methods in compliant mechanisms: An overview. In Proceedings of the International Design Engineering Technical Conferences and Computers and Information in Engineering Conference, San Diego, CA, USA, 30 August–2 September 2009; Volume 7, pp. 193–214. [[CrossRef](#)]
55. Huang, X.; Li, Y.; Zhou, S.; Xie, Y. Topology optimization of compliant mechanisms with desired structural stiffness. *Eng. Struct.* **2014**, *79*, 13–21. [[CrossRef](#)]
56. Pinskiér, J.; Shirinzadeh, B.; Ghafarian, M.; Das, T.K.; Al-Jodah, A.; Nowell, R. Topology optimization of gy optimization of stiffness constrained flexure-hinges for precision and range maximization. *Mech. Mach. Theory* **2020**, *150*, 103874. [[CrossRef](#)]
57. Pinggen, G.; Meyer, D. Topology optimization for thermal transport. In Proceedings of the Fluids Engineering Division Summer Meeting, Vail, CO, USA, 2–6 August 2009; Volume 1, pp. 2237–2243.
58. Nomura, K.; Yamasaki, S.; Yaji, K.; Bo, H.; Takahashi, A.; Kojima, T.; Fujita, K. Topology optimization of conductors in electrical circuit. *Struct. Multidiscip. Optim.* **2019**, *59*, 2205–2225. [[CrossRef](#)]
59. Christensen, J.; de Abajo, F.J.G. Anisotropic metamaterials for full control of acoustic waves. *Phys. Rev. Lett.* **2012**, *108*, 124301. [[CrossRef](#)]
60. Bhate, D.; Penick, C.A.; Ferry, L.A.; Lee, C. Classification and selection of cellular materials in mechanical design: Engineering and biomimetic approaches. *Designs* **2019**, *3*, 19. [[CrossRef](#)]
61. Tamburrino, F.; Graziosi, S.; Bordegoni, M. The Design Process of Additively Manufactured Mesoscale Lattice Structures: A Review. *J. Comput. Inf. Sci. Eng.* **2018**, *18*, 040801. [[CrossRef](#)]
62. Savio, G.; Rosso, S.; Meneghello, R.; Concheri, G. Geometric Modeling of Cellular Materials for Additive Manufacturing in Biomedical Field: A Review. *Appl. Bionics Biomech.* **2018**, *2018*, 14. [[CrossRef](#)]
63. Bhate, D. Lattice Design Optimization: Crowdsourcing Ideas in the Classroom. In Proceedings of the 2018 Annual International Solid Freeform Fabrication Symposium, Austin, TX, USA, 13–15 August 2018; pp. 12–14.
64. Schaedler, T.A.; Carter, W.B. Architected cellular materials. *Annu. Rev. Mater. Res.* **2016**, *46*, 187–210. [[CrossRef](#)]
65. Nguyen, J.; Park, S.I.; Rosen, D.W. Cellular structure design for lightweight components. In *Innovative Developments in Virtual and Physical Prototyping*; Taylor & Francis: Abingdon, UK, 2012; pp. 203–210.
66. Kantareddy, S.; Roh, B.; Simpson, T.; Joshi, S.; Dickman, C.; Lehtihet, E. Saving weight with metallic lattice structures: Design challenges with a real-world example. In Proceedings of the Solid Freeform Fabrication Symposium (SFF), Austin, TX, USA, 8–10 August 2016; pp. 8–10.
67. Cheng, L.; Zhang, P.; Biyikli, E.; Bai, J.; Robbins, J.; To, A. Efficient design optimization of variable-density cellular structures for additive manufacturing: Theory and experimental validation. *Rapid Prototyp. J.* **2017**, *23*, 660–677. [[CrossRef](#)]
68. Chen, W.; Zheng, X.; Liu, S. Finite-element-mesh based method for modeling and optimization of lattice structures for additive manufacturing. *Materials* **2018**, *11*, 2073. [[CrossRef](#)] [[PubMed](#)]

69. Gibson, L.J.; Ashby, M.F. *Cellular Solids: Structure and Properties*; Cambridge University Press: Cambridge, UK, 1999.
70. Bhate, D. Four questions in cellular material design. *Materials* **2019**, *12*, 1060. [[CrossRef](#)] [[PubMed](#)]
71. Benedetti, M.; du Plessis, A.; Ritchie, R.; Dallago, M.; Razavi, S.; Berto, F. Architected cellular materials: A review on their mechanical properties towards fatigue-tolerant design and fabrication. *Mater. Sci. Eng. R Rep.* **2021**, *144*, 100606. [[CrossRef](#)]
72. Cuan-Urquizo, E.; Espinoza-Camacho, J.I.; Álvarez-Trejo, A.; Uribe, E.; Treviño-Quintanilla, C.D.; Crespo-Sánchez, S.E.; Gómez-Espinosa, A.; Roman-Flores, A.; Olvera-Silva, O. Elastic response of lattice arc structures fabricated using curved-layered fused deposition modeling. *Mech. Adv. Mater. Struct.* **2019**, 1–11. [[CrossRef](#)]
73. Rosso, S.; Uriati, F.; Grigolato, L.; Meneghello, R.; Concheri, G.; Savio, G. An Optimization Workflow in Design for Additive Manufacturing. *Appl. Sci.* **2021**, *11*. [[CrossRef](#)]
74. Nazir, A.; Abate, K.M.; Kumar, A.; Jeng, J.-Y. A state-of-the-art review on types, design, optimization, and additive manufacturing of cellular structures. *Int. J. Adv. Manuf. Technol.* **2019**, *104*, 3489–3510. [[CrossRef](#)]
75. Askari, M.; Hutchins, D.A.; Thomas, P.J.; Astolfi, L.; Watson, R.L.; Abdi, M.; Ricci, M.; Laureti, S.; Nie, L.; Freear, S.; et al. Additive manufacturing of metamaterials: A review. *Addit. Manuf.* **2020**, *36*, 101562. [[CrossRef](#)]
76. Chen, L.M.; Chen, M.J.; Pei, Y.M.; Zhang, Y.H.; Fang, D.N. Optimal design of sandwich beams with lightweight cores in three-point bending. *Int. J. Appl. Mech.* **2012**, *4*, 1250033. [[CrossRef](#)]
77. Potes, F.; Silva, J.; Gamboa, P. Development and characterization of a natural lightweight composite solution for aircraft structural applications. *Compos. Struct.* **2016**, *136*, 430–440. [[CrossRef](#)]
78. Cuan-Urquizo, E.; Shalchy, F.; Bhaskar, A. Compressive stiffness of staggered woodpile lattices: Mechanics, measurement, and scaling laws. *Int. J. Mech. Sci.* **2020**, *187*, 105932. [[CrossRef](#)]
79. Chu, J.; Engelbrecht, S.; Graf, G.; Rosen, D.W. A comparison of synthesis methods for cellular structures with application to additive manufacturing. *Rapid Prototyp. J.* **2010**, *16*, 275–283. [[CrossRef](#)]
80. Dragoni, E. Optimal mechanical design of tetrahedral truss cores for sandwich constructions. *J. Sandw. Struct. Mater.* **2013**, *15*, 464–484. [[CrossRef](#)]
81. Leary, M.; Mazur, M.; Elambasseril, J.; McMillan, M.; Chirent, T.; Sun, Y.; Qian, M.; Easton, M.; Brandt, M. Selective laser melting (SLM) of AlSi12Mg lattice structures. *Mater. Des.* **2016**, *98*, 344–357. [[CrossRef](#)]
82. Maskery, I.; Aremu, A.; Parry, L.; Wildman, R.; Tuck, C.; Ashcroft, I. Effective design and simulation of surface-based lattice structures featuring volume fraction and cell type grading. *Mater. Des.* **2018**, *155*, 220–232. [[CrossRef](#)]
83. Weisgraber, T.H.; Metz, T.; Spadaccini, C.M.; Duoss, E.B.; Small, W.; Lenhardt, J.M.; Maxwell, R.S.; Wilson, T.S. A mechanical reduced order model for elastomeric 3D printed architectures. *J. Mater. Res.* **2018**, *33*, 309–316. [[CrossRef](#)]
84. Wang, Y.; Groen, J.P.; Sigmund, O. Simple optimal lattice structures for arbitrary loadings. *Extrem. Mech. Lett.* **2019**, *29*, 100447. [[CrossRef](#)]
85. Álvarez Trejo, A.; Cuan-Urquizo, E.; Roman-Flores, A.; Trapaga-Martinez, L.; Alvarado-Orozco, J. Bézier-based metamaterials: Synthesis, mechanics and additive manufacturing. *Mater. Des.* **2021**, *199*, 109412. [[CrossRef](#)]
86. Trifale, N.T.; Nauman, E.A.; Yazawa, K. Systematic generation, analysis, and characterization of 3D micro-architected metamaterials. *ACS Appl. Mater. Interfaces* **2016**, *8*, 35534–35544. [[CrossRef](#)]
87. Niknam, H.; Akbarzadeh, A.; Rodrigue, D.; Therriault, D. Architected multi-directional functionally graded cellular plates. *Mater. Des.* **2018**, *148*, 188–202. [[CrossRef](#)]
88. Tancogne-Dejean, T.; Mohr, D. Elastically-isotropic elementary cubic lattices composed of tailored hollow beams. *Extrem. Mech. Lett.* **2018**, *22*, 13–18. [[CrossRef](#)]
89. Kim, K.; Heo, H.; Ju, J. A mechanism-based architected material: A hierarchical approach to design Poisson's ratio and stiffness. *Mech. Mater.* **2018**, *125*, 14–25. [[CrossRef](#)]
90. Chen, W.; Watts, S.; Jackson, J.A.; Smith, W.L.; Tortorelli, D.A.; Spadaccini, C.M. Stiff isotropic lattices beyond the Maxwell criterion. *Sci. Adv.* **2019**, *5*, eaaw1937. [[CrossRef](#)] [[PubMed](#)]
91. Tanaka, H. Bi-stiffness property of motion structures transformed into square cells. *Proc. R. Soc. A Math. Phys. Eng. Sci.* **2013**, *469*, 20130063. [[CrossRef](#)]
92. Mihai, L.A.; Alayyash, K.; Wyatt, H. The optimal density of cellular solids in axial tension. *Comput. Methods Biomech. Biomed. Eng.* **2017**, *20*, 701–713. [[CrossRef](#)]
93. Lubombo, C.; Huneault, M.A. Effect of infill patterns on the mechanical performance of lightweight 3D-printed cellular PLA parts. *Mater. Today Commun.* **2018**, *17*, 214–228. [[CrossRef](#)]
94. Wang, H.; Chen, Y.; Rosen, D.W. A hybrid geometric modeling method for large scale conformal cellular structures. In Proceedings of the International Design Engineering Technical Conferences and Computers and Information in Engineering Conference, Long Beach, CA, USA, 24–28 September 2005; Volume 3, pp. 421–427. [[CrossRef](#)]
95. Wang, R.; Shang, J.; Li, X.; Wang, Z.; Luo, Z. Novel topological design of 3D Kagome structure for additive manufacturing. *Rapid Prototyp. J.* **2018**, *24*, 261–269. [[CrossRef](#)]
96. Tancogne-Dejean, T.; Li, X.; Diamantopoulou, M.; Roth, C.; Mohr, D. High strain rate response of additively-manufactured plate-lattices: Experiments and modeling. *J. Dyn. Behav. Mater.* **2019**, *5*, 361–375. [[CrossRef](#)]
97. Qiao, P.; Fan, W.; Davalos, J.F.; Zou, G. Optimization of transverse shear moduli for composite honeycomb cores. *Compos. Struct.* **2008**, *85*, 265–274. [[CrossRef](#)]

98. Fan, W.; Qiao, P.; Davalos, J.F. Design Optimization of Honeycomb Core Configurations for Effective Transverse Shear Stiffness. In Proceedings of the Earth & Space 2008: Engineering, Science, Construction, and Operations in Challenging Environments, Long Beach, CA, USA, 3–5 March 2008; pp. 1–8.
99. Nazir, A.; Arshad, A.B.; Jeng, J.Y. Buckling and Post-Buckling Behavior of Uniform and Variable-Density Lattice Columns Fabricated Using Additive Manufacturing. *Materials* **2019**, *12*, 3539. [[CrossRef](#)]
100. Lipperman, F.; Fuchs, M.B.; Ryvkin, M. Stress localization and strength optimization of frame material with periodic microstructure. *Comput. Methods Appl. Mech. Eng.* **2008**, *197*, 4016–4026. [[CrossRef](#)]
101. Injeti, S.S.; Daraio, C.; Bhattacharya, K. Metamaterials with engineered failure load and stiffness. *Proc. Natl. Acad. Sci. USA* **2019**, *116*, 23960–23965. [[CrossRef](#)] [[PubMed](#)]
102. Parthasarathy, J.; Starly, B.; Raman, S. A design for the additive manufacture of functionally graded porous structures with tailored mechanical properties for biomedical applications. *J. Manuf. Process.* **2011**, *13*, 160–170. [[CrossRef](#)]
103. Kim, K.; Ju, J.; Kim, D.M. Cellular materials with extremely high negative and positive Poisson's ratios: A mechanism based material design. In Proceedings of the ASME International Mechanical Engineering Congress and Exposition, San Diego, CA, USA, 15–21 November 2013; American Society of Mechanical Engineers: New York, NY, USA, 2013; Volume 9, p. V009T10A045, [[CrossRef](#)]
104. Kim, K.; Ju, J.; Kim, D.M. Porous materials with high negative Poisson's ratios—A mechanism based material design. *Smart Mater. Struct.* **2013**, *22*, 084007. [[CrossRef](#)]
105. Novak, N.; Vesenjok, M.; Ren, Z. Auxetic cellular materials—a review. *Stroj. Vestn. J. Mech. Eng.* **2016**, *62*, 485–493. [[CrossRef](#)]
106. Duoss, E.B.; Weisgraber, T.H.; Hearon, K.; Zhu, C.; Small IV, W.; Metz, T.R.; Vericella, J.J.; Barth, H.D.; Kuntz, J.D.; Maxwell, R.S.; et al. Three-dimensional printing of elastomeric, cellular architectures with negative stiffness. *Adv. Funct. Mater.* **2014**, *24*, 4905–4913. [[CrossRef](#)]
107. Neff, C.; Hopkinson, N.; Crane, N.B. Selective laser sintering of diamond lattice structures: Experimental results and FEA model comparison. *Solid Free Fabr.* **2015**, *25*, 1104.
108. Runkel, F.; Molinari, G.; Arrieta, A.F.; Ermanni, P. Tailorable stiffness chiral metastructure. *Phys. Status Solidi RRL Rapid Res. Lett.* **2017**, *11*, 1700233. [[CrossRef](#)]
109. Ion, A.; Frohnhofen, J.; Wall, L.; Kovacs, R.; Alistar, M.; Lindsay, J.; Lopes, P.; Chen, H.T.; Baudisch, P. Metamaterial mechanisms. In Proceedings of the 29th Annual Symposium on User Interface Software and Technology, Tokyo, Japan, 16–19 October 2016; pp. 529–539.
110. Ou, J.; Ma, Z.; Peters, J.; Dai, S.; Vlavianos, N.; Ishii, H. KinetiX—Designing auxetic-inspired deformable material structures. *Comput. Graph.* **2018**, *75*, 72–81. [[CrossRef](#)]
111. Soltani, Z.; Santer, M. The determination and enhancement of compliant modes for high-amplitude actuation in lattices. *Int. J. Solids Struct.* **2020**, *206*, 124–136. [[CrossRef](#)]
112. Dunn, M.; Wheel, M. Size effect anomalies in the behaviour of loaded 3D mechanical metamaterials. *Philos. Mag.* **2020**, *100*, 139–156. [[CrossRef](#)]
113. Gong, X.; Huang, J.; Scarpa, F.; Liu, Y.; Leng, J. Zero Poisson's ratio cellular structure for two-dimensional morphing applications. *Compos. Struct.* **2015**, *134*, 384–392. [[CrossRef](#)]
114. Liu, W.; Li, H.; Zhang, J.; Bai, Y. In-plane mechanics of a novel cellular structure for multiple morphing applications. *Compos. Struct.* **2019**, *207*, 598–611. [[CrossRef](#)]
115. Liu, W.; Li, H.; Yang, Z.; Zhang, J.; Xiong, C. Mechanics of a novel cellular structure for morphing applications. *Aerosp. Sci. Technol.* **2019**, *95*, 105479. [[CrossRef](#)]
116. Bornengo, D.; Scarpa, F.; Remillat, C. Evaluation of hexagonal chiral structure for morphing airfoil concept. *Proc. Inst. Mech. Eng. Part G J. Aerosp. Eng.* **2005**, *219*, 185–192. [[CrossRef](#)]
117. Dong, W.J.; Sun, Q. A Novel Basic Conceptual Design and Analysis of a Morphing Wing Using Re-Entrant Hexagonal Cellular Structure. *Adv. Mater. Res.* **2011**, *308*, 548–552. [[CrossRef](#)]
118. Zhang, P.; Zhou, L.; Qiu, T. Design and application of cross-shaped cellular honeycombs for a variable camber wing. *J. Aircr.* **2012**, *49*, 1451–1459. [[CrossRef](#)]
119. Heo, H.; Ju, J.; Kim, D.M. Compliant cellular structures: Application to a passive morphing airfoil. *Compos. Struct.* **2013**, *106*, 560–569. [[CrossRef](#)]
120. Olympio, K.R.; Gandhi, F. Flexible skins for morphing aircraft using cellular honeycomb cores. *J. Intell. Mater. Syst. Struct.* **2010**, *21*, 1719–1735. [[CrossRef](#)]
121. Olympio, K.; Gandhi, F. Zero- ν cellular honeycomb flexible skins for one-dimensional wing morphing. In Proceedings of the 48th AIAA/ASME/ASCE/AHS/ASC Structures, Structural Dynamics, and Materials Conference, Honolulu, HI, USA, 23–26 April 2007; p. 1735, [[CrossRef](#)]
122. Chen, J.; Shen, X.; Li, J. Zero Poisson's ratio flexible skin for potential two-dimensional wing morphing. *Aerosp. Sci. Technol.* **2015**, *45*, 228–241. [[CrossRef](#)]
123. Vigliotti, A.; Pasini, D. Analysis and design of lattice materials for large cord and curvature variations in skin panels of morphing wings. *Smart Mater. Struct.* **2015**, *24*, 037006. [[CrossRef](#)]
124. Chang, L.; Shen, X. Design of cellular based structures in sandwiched morphing skin via topology optimization. *Struct. Multidiscip. Optim.* **2018**, *58*, 2085–2098. [[CrossRef](#)]
125. Naghavi Zadeh, M.; Dayyani, I.; Yasaee, M. Fish Cells, a new zero Poisson's ratio metamaterial—Part I: Design and experiment. *J. Intell. Mater. Syst. Struct.* **2020**, *31*, 1617–1637. [[CrossRef](#)]

126. Zadeh, M.N.; Dayyani, I.; Yasaee, M. Fish Cells, a new zero Poisson's ratio metamaterial—Part II: Elastic properties. *J. Intell. Mater. Syst. Struct.* **2020**, *31*, 2196–2210. [[CrossRef](#)]
127. Jenett, B.; Calisch, S.; Cellucci, D.; Cramer, N.; Gershenfeld, N.; Sweil, S.; Cheung, K.C. Digital morphing wing: Active wing shaping concept using composite lattice-based cellular structures. *Soft Robot.* **2017**, *4*, 33–48. [[CrossRef](#)] [[PubMed](#)]
128. Cramer, N.B.; Cellucci, D.W.; Formoso, O.B.; Gregg, C.E.; Jenett, B.E.; Kim, J.H.; Lendraitis, M.; Sweil, S.S.; Trinh, G.T.; Trinh, K.V.; et al. Elastic shape morphing of ultralight structures by programmable assembly. *Smart Mater. Struct.* **2019**, *28*, 055006. [[CrossRef](#)] [[PubMed](#)]
129. Habib, F.; Iovenitti, P.; Masood, S.; Nikzad, M. Fabrication of polymeric lattice structures for optimum energy absorption using Multi Jet Fusion technology. *Mater. Des.* **2018**, *155*, 86–98. [[CrossRef](#)]
130. Yuan, S.; Chua, C.K.; Zhou, K. 3D-Printed Mechanical Metamaterials with High Energy Absorption. *Adv. Mater. Technol.* **2019**, *4*, 1800419. [[CrossRef](#)]
131. Sarvestani, H.Y.; Akbarzadeh, A.; Mirbolghasemi, A.; Hermenean, K. 3D printed meta-sandwich structures: Failure mechanism, energy absorption and multi-hit capability. *Mater. Des.* **2018**, *160*, 179–193. [[CrossRef](#)]
132. Gao, Q.; Zhao, X.; Wang, C.; Wang, L.; Ma, Z. Multi-objective crashworthiness optimization for an auxetic cylindrical structure under axial impact loading. *Mater. Des.* **2018**, *143*, 120–130. [[CrossRef](#)]
133. Lai, C.Q.; Daraio, C. Highly porous microlattices as ultrathin and efficient impact absorbers. *Int. J. Impact Eng.* **2018**, *120*, 138–149. [[CrossRef](#)]
134. Saxena, K.K.; Calius, E.P.; Das, R. Tailoring cellular auxetics for wearable applications with multimaterial 3D printing. In Proceedings of the ASME International Mechanical Engineering Congress and Exposition, Phoenix, AZ, USA, 11–17 November 2016; American Society of Mechanical Engineers: New York, NY, USA, 2016; Volume 9, p. V009T12A063, [[CrossRef](#)]
135. Izard, A.G.; Alfonso, R.F.; McKnight, G.; Valdevit, L. Optimal design of a cellular material encompassing negative stiffness elements for unique combinations of stiffness and elastic hysteresis. *Mater. Des.* **2017**, *135*, 37–50. [[CrossRef](#)]
136. Wang, B.; Tan, X.; Zhu, S.; Chen, S.; Yao, K.; Xu, P.; Wang, L.; Wu, H.; Sun, Y. Cushion performance of cylindrical negative stiffness structures: Analysis and optimization. *Compos. Struct.* **2019**, *227*, 111276. [[CrossRef](#)]
137. Hyland, J.E.; Frecker, M.I.; Lesieutre, G.A. Optimization of honeycomb contact-Aided compliant cellular mechanism for strain energy absorption. In Proceedings of the International Design Engineering Technical Conferences and Computers and Information in Engineering Conference, Chicago, IL, USA, 12–15 August 2012; American Society of Mechanical Engineers: New York, NY, USA, 2012; Volume 4, pp. 311–320. [[CrossRef](#)]
138. Khurana, J.; Hanks, B.; Frecker, M. Design for additive manufacturing of cellular compliant mechanism using thermal history feedback. In Proceedings of the International Design Engineering Technical Conferences and Computers and Information in Engineering Conference, Quebec City, QC, Canada, 26–29 August 2018; American Society of Mechanical Engineers: New York, NY, USA, 2018; Volume 2A, p. V02AT03A035, [[CrossRef](#)]
139. Han, B.; Zhang, Z.J.; Zhang, Q.C.; Zhang, Q.; Lu, T.J.; Lu, B.H. Recent advances in hybrid lattice-cored sandwiches for enhanced multifunctional performance. *Extrem. Mech. Lett.* **2017**, *10*, 58–69. [[CrossRef](#)]
140. Xu, F.; Zhang, X.; Zhang, H. A review on functionally graded structures and materials for energy absorption. *Eng. Struct.* **2018**, *171*, 309–325. [[CrossRef](#)]
141. San Ha, N.; Lu, G. A review of recent research on bio-inspired structures and materials for energy absorption applications. *Compos. Part B Eng.* **2020**, *181*, 107496. [[CrossRef](#)]
142. Zhang, J.; Lu, G.; You, Z. Large deformation and energy absorption of additively manufactured auxetic materials and structures: A review. *Compos. Part B Eng.* **2020**, 108340. [[CrossRef](#)]
143. van Dijk, N.P.; Maute, K.; Langelaar, M.; Van Keulen, F. Level-set methods for structural topology optimization: A review. *Struct. Multidiscip. Optim.* **2013**, *48*, 437–472. [[CrossRef](#)]
144. Bendsoe, M.P.; Sigmund, O. *Topology Optimization: Theory, Methods, and Applications*; Springer Science & Business Media: Berlin/Heidelberg, Germany, 2013.
145. Bendsoe, M.P. Optimal shape design as a material distribution problem. *Struct. Optim.* **1989**, *1*, 193–202. [[CrossRef](#)]
146. Cadman, J.E.; Zhou, S.; Chen, Y.; Li, Q. On design of multi-functional microstructural materials. *J. Mater. Sci.* **2013**, *48*, 51–66. [[CrossRef](#)]
147. Deaton, J.D.; Grandhi, R.V. A survey of structural and multidisciplinary continuum topology optimization: Post 2000. *Struct. Multidiscip. Optim.* **2014**, *49*, 1–38. [[CrossRef](#)]
148. Sigmund, O.; Maute, K. Topology optimization approaches. *Struct. Multidiscip. Optim.* **2013**, *48*, 1031–1055. [[CrossRef](#)]
149. Huang, X.; Xie, M. *Evolutionary Topology Optimization of Continuum Structures: Methods and Applications*; John Wiley & Sons: Hoboken, NJ, USA, 2010.
150. Subedi, S.C.; Verma, C.S.; Suresh, K. A Review of Methods for the Geometric Post-Processing of Topology Optimized Models. *J. Comput. Inf. Sci. Eng.* **2020**, *20*, 060801. [[CrossRef](#)]
151. Sigmund, O. Design of Material Structures Using Topology Optimization. Ph.D. Thesis, Technical University of Denmark, Lyngby, Denmark, 1994.
152. Eschenauer, H.A.; Olhoff, N. Topology optimization of continuum structures: A review. *Appl. Mech. Rev.* **2001**, *54*, 331–390. [[CrossRef](#)]
153. Sigmund, O. A new class of extremal composites. *J. Mech. Phys. Solids* **2000**, *48*, 397–428. [[CrossRef](#)]

154. Gibiansky, L.V.; Sigmund, O. Multiphase composites with extremal bulk modulus. *J. Mech. Phys. Solids* **2000**, *48*, 461–498. [[CrossRef](#)]
155. Arabnejad, S.; Pasini, D. Mechanical properties of lattice materials via asymptotic homogenization and comparison with alternative homogenization methods. *Int. J. Mech. Sci.* **2013**, *77*, 249–262. [[CrossRef](#)]
156. Neves, M.; Rodrigues, H.; Guedes, J.M. Optimal design of periodic linear elastic microstructures. *Comput. Struct.* **2000**, *76*, 421–429. [[CrossRef](#)]
157. Sigmund, O. Materials with prescribed constitutive parameters: An inverse homogenization problem. *Int. J. Solids Struct.* **1994**, *31*, 2313–2329. [[CrossRef](#)]
158. Sigmund, O. Tailoring materials with prescribed elastic properties. *Mech. Mater.* **1995**, *20*, 351–368. [[CrossRef](#)]
159. Osanov, M.; Guest, J.K. Topology optimization for architected materials design. *Annu. Rev. Mater. Res.* **2016**, *46*, 211–233. [[CrossRef](#)]
160. Song, J.; Wang, Y.; Zhou, W.; Fan, R.; Yu, B.; Lu, Y.; Li, L. Topology optimization-guided lattice composites and their mechanical characterizations. *Compos. Part B Eng.* **2019**, *160*, 402–411. [[CrossRef](#)]
161. Hu, Z.; Gadipudi, V.K.; Salem, D.R. Topology optimization of lightweight lattice structural composites inspired by cuttlefish bone. *Appl. Compos. Mater.* **2019**, *26*, 15–27. [[CrossRef](#)]
162. Zhang, L.; Song, B.; Fu, J.; Wei, S.; Yang, L.; Yan, C.; Li, H.; Gao, L.; Shi, Y. Topology-optimized lattice structures with simultaneously high stiffness and light weight fabrication by selective laser melting: Design, manufacturing and characterization. *J. Manuf. Process.* **2020**, *56*, 1166–1177. [[CrossRef](#)]
163. Du, Y.; Li, H.; Luo, Z.; Tian, Q. Topological design optimization of lattice structures to maximize shear stiffness. *Adv. Eng. Softw.* **2017**, *112*, 211–221. [[CrossRef](#)]
164. Xiao, Z.; Yang, Y.; Xiao, R.; Bai, Y.; Song, C.; Wang, D. Evaluation of topology-optimized lattice structures manufactured via selective laser melting. *Mater. Des.* **2018**, *143*, 27–37. [[CrossRef](#)]
165. Yang, C.; Xu, P.; Xie, S.; Yao, S. Mechanical performances of four lattice materials guided by topology optimisation. *Scr. Mater.* **2020**, *178*, 339–345. [[CrossRef](#)]
166. Challis, V.; Roberts, A.; Wilkins, A. Design of three dimensional isotropic microstructures for maximized stiffness and conductivity. *Int. J. Solids Struct.* **2008**, *45*, 4130–4146. [[CrossRef](#)]
167. Barba, D.; Reed, R.C.; Alabort, E. Design of Metallic Lattices for Bone Implants by Additive Manufacturing. In Proceedings of the TMS 2020 149th Annual Meeting & Exhibition Supplemental Proceedings, San Diego, CA, USA, 23–27 February 2020; pp. 745–759. [[CrossRef](#)]
168. Colabella, L.; Cisilino, A.P.; Fachinotti, V.; Kowalczyk, P. Multiscale design of elastic solids with biomimetic cancellous bone cellular microstructures. *Struct. Multidiscip. Optim.* **2019**, *60*, 639–661. [[CrossRef](#)]
169. Colabella, L.; Cisilino, A.; Fachinotti, V.; Capiel, C.; Kowalczyk, P. Multiscale design of artificial bones with biomimetic elastic microstructures. *J. Mech. Behav. Biomed. Mater.* **2020**, *108*, 103748. [[CrossRef](#)]
170. Sutradhar, A.; Paulino, G.H.; Miller, M.J.; Nguyen, T.H. Topological optimization for designing patient-specific large craniofacial segmental bone replacements. *Proc. Natl. Acad. Sci. USA* **2010**, *107*, 13222–13227. [[CrossRef](#)] [[PubMed](#)]
171. Panesar, A.; Abdi, M.; Hickman, D.; Ashcroft, I. Strategies for functionally graded lattice structures derived using topology optimisation for additive manufacturing. *Addit. Manuf.* **2018**, *19*, 81–94. [[CrossRef](#)]
172. Wang, Y.; Zhang, L.; Daynes, S.; Zhang, H.; Feih, S.; Wang, M.Y. Design of graded lattice structure with optimized mesostructures for additive manufacturing. *Mater. Des.* **2018**, *142*, 114–123. [[CrossRef](#)]
173. Zhang, H.; Wang, Y.; Kang, Z. Topology optimization for concurrent design of layer-wise graded lattice materials and structures. *Int. J. Eng. Sci.* **2019**, *138*, 26–49. [[CrossRef](#)]
174. Xia, L.; Breitkopf, P. Concurrent topology optimization design of material and structure within FE2 nonlinear multiscale analysis framework. *Comput. Methods Appl. Mech. Eng.* **2014**, *278*, 524–542. [[CrossRef](#)]
175. Qiu, W.; Jin, P.; Jin, S.; Wang, C.; Xia, L.; Zhu, J.; Shi, T. An Evolutionary Design Approach to Shell-infill Structures. *Addit. Manuf.* **2020**, *34*, 101382. [[CrossRef](#)]
176. Jin, X.; Li, G.X.; Zhang, M. Design and optimization of nonuniform cellular structures. *Proc. Inst. Mech. Eng. Part C J. Mech. Eng. Sci.* **2018**, *232*, 1280–1293. [[CrossRef](#)]
177. Liu, P.; Kang, Z.; Luo, Y. Two-scale concurrent topology optimization of lattice structures with connectable microstructures. *Addit. Manuf.* **2020**, *36*, 101427. [[CrossRef](#)]
178. Seyedkanani, A.; Niknam, H.; Akbarzadeh, A. Bending Behavior of Optimally Graded 3D Printed Cellular Beams. *Addit. Manuf.* **2020**, *35*, 101327. [[CrossRef](#)]
179. Jia, J.; Da, D.; Loh, C.L.; Zhao, H.; Yin, S.; Xu, J. Multiscale topology optimization for non-uniform microstructures with hybrid cellular automata. *Struct. Multidiscip. Optim.* **2020**, *62*, 757–770. [[CrossRef](#)]
180. Kang, D.; Park, S.; Son, Y.; Yeon, S.; Kim, S.H.; Kim, I. Multi-lattice inner structures for high-strength and light-weight in metal selective laser melting process. *Mater. Des.* **2019**, *175*, 107786. [[CrossRef](#)]
181. Li, D.; Liao, W.; Dai, N.; Xie, Y.M. Anisotropic design and optimization of conformal gradient lattice structures. *Comput. Aided Des.* **2020**, *119*, 102787. [[CrossRef](#)]
182. Radman, A.; Huang, X.; Xie, Y. Topology optimization of functionally graded cellular materials. *J. Mater. Sci.* **2013**, *48*, 1503–1510. [[CrossRef](#)]

183. Bharanidaran, R.; Ramesh, T. Numerical simulation and experimental investigation of a topologically optimized compliant microgripper. *Sens. Actuators A Phys.* **2014**, *205*, 156–163. [[CrossRef](#)]
184. Clark, L.; Shirinzadeh, B.; Pinski, J.; Tian, Y.; Zhang, D. Topology optimisation of bridge input structures with maximal amplification for design of flexure mechanisms. *Mech. Mach. Theory* **2018**, *122*, 113–131. [[CrossRef](#)]
185. Ramesh, T.; Bharanidaran, R.; Gopal, V. Design and development of XY Micro-Positioning Stage Using Modified Topology Optimization Technique. *Appl. Mech. Mater.* **2014**, *592*, 2220–2224. [[CrossRef](#)]
186. Wang, J.X.; Guo, W.Z. The Topology Optimization of Controllable Path-Generating Compliant Mechanisms. *J. Shanghai Jiaotong Univ.* **2006**, *6*.
187. Bharanidaran, R.; Ramesh, T. A modified post-processing technique to design a compliant based microgripper with a plunger using topological optimization. *Int. J. Adv. Manuf. Technol.* **2017**, *93*, 103–112. [[CrossRef](#)]
188. Olympio, K.R.; Gandhi, F. Optimal cellular core topologies for one-dimensional morphing aircraft structures. *J. Mech. Des.* **2012**, *134*, 081005. [[CrossRef](#)]
189. Chang, L.; Shen, X.; Dai, Y.; Wang, T.; Zhang, L. Investigation on the mechanical properties of topologically optimized cellular structures for sandwiched morphing skins. *Compos. Struct.* **2020**, *250*, 112555. [[CrossRef](#)]
190. Gomes, P.; Palacios, R. Aerodynamic-driven topology optimization of compliant airfoils. *Struct. Multidiscip. Optim.* **2020**, *62*, 2117–2130. [[CrossRef](#)]
191. Zhang, Z.; Song, C.; Yang, C.; Cavalieri, V.; De Gaspari, A.; Ricci, S. Combining Density-based Approach and Optimization Refinement in the Design of Morphing Airfoil Structures. In Proceedings of the AIAA Scitech 2020 Forum, Orlando, FL, USA, 6–10 January 2020; p. 1546, [[CrossRef](#)]
192. Liu, Y.; Li, S.; Zhang, L.; Hao, Y.; Sercombe, T. Early plastic deformation behaviour and energy absorption in porous β -type biomedical titanium produced by selective laser melting. *Scr. Mater.* **2018**, *153*, 99–103. [[CrossRef](#)]
193. Deng, H.; Cheng, L.; Liang, X.; Hayduke, D.; To, A.C. Topology optimization for energy dissipation design of lattice structures through snap-through behavior. *Comput. Methods Appl. Mech. Eng.* **2020**, *358*, 112641. [[CrossRef](#)]
194. Najmon, J.; DeHart, J.; Wood, Z.; Tovar, A. Development of a Helmet Liner Through Bio-Inspired Structures and Topology Optimized Compliant Mechanism Arrays. *SAE Int. J. Trans. Safety* **2018**, *6*, 217–235. [[CrossRef](#)]
195. Borovinšek, M.; Novak, N.; Vesenj, M.; Ren, Z.; Ulbin, M. Designing 2D auxetic structures using multi-objective topology optimization. *Mater. Sci. Eng. A* **2020**, *795*, 139914. [[CrossRef](#)]
196. de Lima, C.R.; Paulino, G.H. Auxetic structure design using compliant mechanisms: A topology optimization approach with polygonal finite elements. *Adv. Eng. Softw.* **2019**, *129*, 69–80. [[CrossRef](#)]
197. Kaminakis, N.T.; Drosopoulos, G.A.; Stavroulakis, G.E. Design and verification of auxetic microstructures using topology optimization and homogenization. *Arch. Appl. Mech.* **2015**, *85*, 1289–1306. [[CrossRef](#)]
198. Andreassen, E.; Lazarov, B.S.; Sigmund, O. Design of manufacturable 3D extremal elastic microstructure. *Mech. Mater.* **2014**, *69*, 1–10. [[CrossRef](#)]
199. Deng, H.; Hinnebusch, S.; To, A.C. Topology optimization design of stretchable metamaterials with Bézier skeleton explicit density (BSED) representation algorithm. *Comput. Methods Appl. Mech. Eng.* **2020**, *366*, 113093. [[CrossRef](#)]
200. Lum, G.Z.; Teo, T.J.; Yeo, S.H.; Yang, G.; Sitti, M. Structural optimization for flexure-based parallel mechanisms—Towards achieving optimal dynamic and stiffness properties. *Precis. Eng.* **2015**, *42*, 195–207. [[CrossRef](#)]
201. Jin, M.; Zhang, X. A new topology optimization method for planar compliant parallel mechanisms. *Mech. Mach. Theory* **2016**, *95*, 42–58. [[CrossRef](#)]
202. Jin, M.; Zhang, X.; Yang, Z.; Zhu, B. Jacobian-based topology optimization method using an improved stiffness evaluation. *J. Mech. Des.* **2018**, *140*, 011402. [[CrossRef](#)]
203. Zhan, W.; He, X.; Yang, J.; Lai, J.; Zhu, D. Optimal design method for 3-DOF planar compliant mechanisms based on mapping matrix constraints. *Structures* **2020**, *26*, 1–5. [[CrossRef](#)]
204. Wang, G.; Zhu, D.; Liu, N.; Zhao, W. Multi-objective topology optimization of a compliant parallel planar mechanism under combined load cases and constraints. *Micromachines* **2017**, *8*, 279. [[CrossRef](#)] [[PubMed](#)]
205. Zhu, D.; Zhang, C.; Feng, Y. Topological Structure Synthesis of Three-Rotational-DOF Compliant Mechanisms. In Proceedings of the 2018 IEEE International Conference on Manipulation, Manufacturing and Measurement on the Nanoscale (3M-NANO), Hangzhou, China, 13–17 August 2018; IEEE: Piscataway, NJ, USA, 2018; pp. 304–307. [[CrossRef](#)]
206. Zhu, D.; Feng, Y.; Zhan, W. Topology optimization of three-translational degree-of-freedom spatial compliant mechanism. *Adv. Mech. Eng.* **2019**, *11*, 1–12. [[CrossRef](#)]
207. Zhu, B.; Zhang, X.; Fatikow, S. Design of single-axis flexure hinges using continuum topology optimization method. *Sci. China Technol. Sci.* **2014**, *57*, 560–567. [[CrossRef](#)]
208. Zhu, B.; Liu, M.; Chen, Q.; Li, H.; Zhang, X.; Fu, Y. Topology optimization of the flexure hinges for precision engineering. In Proceedings of the 2017 International Conference on Manipulation, Automation and Robotics at Small Scales (MARSS), Montreal, QC, Canada, 17–21 July 2017; IEEE: Piscataway, NJ, USA, 2017; pp. 1–5. [[CrossRef](#)]
209. Zhu, B.; Zhang, X.; Liu, M.; Chen, Q.; Li, H. Topological and shape optimization of flexure hinges for designing compliant mechanisms using the level set method. *Chin. J. Mech. Eng.* **2019**, *32*, 13. [[CrossRef](#)]
210. Liu, M.; Zhang, X.; Fatikow, S. Topology optimization of large-displacement flexure hinges. In Proceedings of the International Design Engineering Technical Conferences and Computers and Information in Engineering Conference, Boston, MA, USA, 2–5 August 2015; American Society of Mechanical Engineers: New York, NY, USA, 2015; Volume 5A, p. V05AT08A005, [[CrossRef](#)]

211. Liu, M.; Zhang, X.; Fatikow, S. Design and analysis of a high-accuracy flexure hinge. *Rev. Sci. Instrum.* **2016**, *87*, 055106, [[CrossRef](#)]
212. Liu, M.; Zhang, X.; Fatikow, S. Design of flexure hinges based on stress-constrained topology optimization. *Proc. Inst. Mech. Eng. Part C J. Mech. Eng. Sci.* **2017**, *231*, 4635–4645. [[CrossRef](#)]
213. Liu, M.; Zhan, J.; Zhu, B.; Zhang, X. Topology Optimization of Flexure Hinges with Distributed Stress for Flexure-Based Mechanisms. In Proceedings of the 2018 International Conference on Manipulation, Automation and Robotics at Small Scales (MARSS), Nagoya, Japan, 4–8 July 2018; IEEE: Piscataway, NJ, USA, 2018; pp. 1–5. [[CrossRef](#)]
214. Liu, M.; Zhan, J.; Zhang, X. Topology optimization of distributed flexure hinges with desired performance. *Eng. Optim.* **2020**, *52*, 405–425. [[CrossRef](#)]
215. Liu, M.; Zhang, X.; Fatikow, S. Design and analysis of a multi-notched flexure hinge for compliant mechanisms. *Precis. Eng.* **2017**, *48*, 292–304. [[CrossRef](#)]
216. Lobontiu, N.; Cullin, M. In-plane elastic response of two-segment circular-axis symmetric notch flexure hinges: The right circular design. *Precis. Eng.* **2013**, *37*, 542–555. [[CrossRef](#)]
217. Lobontiu, N.; Paine, J.S.; Garcia, E.; Goldfarb, M. Corner-filletted flexure hinges. *J. Mech. Des.* **2001**, *123*, 346–352. [[CrossRef](#)]
218. Smith, S.T.; Badami, V.G.; Dale, J.S.; Xu, Y. Elliptical flexure hinges. *Rev. Sci. Instrum.* **1997**, *68*, 1474–1483. [[CrossRef](#)]
219. Lobontiu, N.; Paine, J.S.; O'Malley, E.; Samuelson, M. Parabolic and hyperbolic flexure hinges: Flexibility, motion precision and stress characterization based on compliance closed-form equations. *Precis. Eng.* **2002**, *26*, 183–192. [[CrossRef](#)]
220. Qiu, L.; Yue, X.; Xie, Z. Design and analysis of Multicavity Flexure Hinge (MCFH) based on three-dimensional continuum topology optimization. *Mech. Mach. Theory* **2019**, *139*, 21–33. [[CrossRef](#)]
221. Qiu, L.; Yue, X.; Zheng, L.; Li, Y. Design and analysis of porous flexure hinge based on dual-objective topology optimization of three-dimensional continuum. *J. Braz. Soc. Mech. Sci. Eng.* **2020**, *42*. [[CrossRef](#)]
222. Li, L.; Geng, Z.; Zhong, B. Design and Optimization of Compliant Revolute Joint Based on Finite Element Method. In *Intelligent Computing, Networked Control, and Their Engineering Applications*; Springer: Berlin/Heidelberg, Germany, 2017; pp. 115–124. [[CrossRef](#)]
223. Li, L.; Geng, Z.; Zhu, X. Experimental and numerical investigation of a large stroke compliant revolute joint. *Microsyst. Technol.* **2019**, *25*, 925–935. [[CrossRef](#)]
224. Li, L.; Zhu, X. Design of compliant revolute joints based on mechanism stiffness matrix through topology optimization using a parameterization level set method. *Struct. Multidiscip. Optim.* **2019**, *60*, 1475–1489. [[CrossRef](#)]